

A time-frequency approach to relativistic correlations in quantum field theory

Benjamin Roussel^{1,*} and Alexandre Feller^{1,†}

¹*Advanced Concepts Team, European Space Agency, Noordwijk, 2201 AZ, Netherlands*

Moving detectors in relativistic quantum field theories reveal the fundamental entangled structure of the vacuum which manifests, for instance, through its thermal character when probed by a uniformly accelerated detector. In this paper, we propose a general formalism inspired both from signal processing and correlation functions of quantum optics to analyze the response of point-like detectors following a generic, non-stationary trajectory. In this context, the Wigner representation of the first-order correlation of the quantum field is a natural time-frequency tool to understand single-detection events. This framework offers a synthetic perspective on the problem of detection in relativistic theory and allows us to analyze various non-stationary situations (adiabatic, periodic) and how excitations and superpositions are deformed by motion. It opens up interesting perspective on the issue of the definition of particles.

I. INTRODUCTION

One of the fundamental differences between relativistic quantum field theories and quantum mechanics is the deeply entangled structure of quantum fields. While this can be understood in a general formal setting [1, 2], one of the clearest phenomena illustrating this is the entangled structure of the vacuum state which is revealed by its thermal character in curved spacetime [3] or by a uniformly accelerated observer [4], respectively known as the Hawking and Unruh effects.

The correlated nature of the vacuum is nicely probed by considering a moving detector in spacetime coupled to the quantum field. Such models are known as Unruh-Dewitt detectors. The thermal nature of the vacuum is then seen through its photo-detection response. Many questions can then be addressed such as the role of causality [5], the behavior under different motions [6–8] or the effect of the switching function of the detector [9, 10]. A similar photo-detection approach has been used in quantum optic since the work of Glauber on coherence functions [11, 12] and has been extended to condensed matter situations [13].

However, the interpretation of these responses in the context of relativistic quantum field theory in flat or in curved spacetime is subtler than in quantum optics since no general notion of particles can be defined in the standard way. The qualitative reason comes from the non existence of a global definition of time. Two directions can then be taken. The first direction is to have an operational perspective: particles are defined through the response signal of the detector itself [4]. The second direction follows a more pragmatic interpretation of the detector’s response: the detector is simply seen as a “fluctuometer”, as a system that responds to the fluctuations of the quantum field. The signal should not *a priori* be interpreted as coming from a particle content [6, 14, 15].

Following this latter point of view is similar to adopt a signal processing perspective, which we will adopt here. In a non stationary context, physically meaningful information can be extracted from the signal by performing a time-frequency analysis, giving us access to the evolution in time of the frequency content of the response. Time-frequency (or time-scale) analysis is now a major tool in signal processing, especially the Wigner function distribution [16]. Historically, the Wigner function has been introduced in quantum mechanics as a phase space representation of the quantum state [17]. This distribution is now widely used in quantum optics [18] and has been recently adapted to analyze coherence properties of electron in the quantum Hall regime [19, 20].

In this paper, we present a unified view on the response of a moving detector probing a relativistic quantum field using a time-frequency approach of the correlation functions of the field based on the Wigner distribution. The main goal is to introduce the a good framework to analyze the response of a detector in general situations where the state of the field can contain excitations, for an arbitrary trajectory. This is achieved by using both the correlation functions formalism and a time-frequency analysis. Physically realistic situations can then be analyzed quantitatively through analytical and numerical computations. Having a time-frequency analysis and a quantum optics perspective on the problem of relativistic detector response provides a synthetic approach to the problem of moving detectors. Besides, this time-frequency perspective sheds new lights on the interpretation of the measured signal and the problem of defining a notion of particles. Indeed, having two natural ways of defining particles, the standard many-body one and the operational one, demands to relate them and understand their interplay. Time-frequency analysis offers a way to define relative stationary timescales from which notions of particles can be defined locally in spacetime and frequency domains.

This paper is structured as follows. In Sec. II we set up the general framework of correlation functions and their time-frequency representation through the Wigner function. In Sec. III, we analyze the response of a detector

*Electronic address: benjamin.roussel@esa.int

†Electronic address: alexandre.feller@esa.int

probing the vacuum for different non-stationary motions of the detector. We give a detailed analysis of the adiabatic regime, its corrections and its breakdown. Sec. IV is dedicated to the study of the detector's response in the presence of excitations in the uniformly accelerated and realistic motions. In particular, how coherences in a superposition transform can be analyzed straightforwardly. We conclude this paper in Sec. V by discussing how different notions of particles can be defined from the signal from a time-frequency analysis.

II. FIRST ORDER CORRELATION

A. Context and photo-detection

Systems in quantum optics, condensed matter and high-energy physics are well described using the framework of quantum field theories. In this context, the experimentally relevant quantities are not the fields themselves but correlations functions constructed from them. Some of them are known in quantum optics as coherence or Glauber functions. They naturally come by when analyzing the photo-detection response.

We are also here interested in the photo-detection response of a system moving arbitrarily in flat spacetime. It is designed to detect a single excitation of a relativistic quantum field. We suppose that this device is moving in Minkowski spacetime with a given trajectory $\mathbf{x}(\tau)$ and is coupled linearly to a massless scalar field $\phi(x)$. In the inertial laboratory reference frame the Hamiltonian is given in the interaction picture by:

$$H_I(\tau) = d(\tau) \cdot \phi^{(I)}(t(\tau), \mathbf{x}(\tau)). \quad (1)$$

If we model the detector as a two level system of energy ω_{eg} , then $d(\tau) = -g\sigma_x(\tau)$ with g the coupling constant.

We are now interested in the probability to measure the excited state after a time τ . Since the coupling is weak, we can use time-dependent perturbation theory, expand the evolution operator at the first order and obtain the desired probability $p_{\omega_{eg}}(\tau)$:

$$p_{\omega_{eg}}(\tau) = \left(\frac{g}{\hbar}\right)^2 \int_0^\tau e^{i\omega_{eg}(\tau_1 - \tau_2)} G(\tau_1, \tau_2) d\tau_1 d\tau_2. \quad (2)$$

The function $G(\tau_1, \tau_2)$ depends only on the state of the scalar field and is defined as a first order correlation function:

$$G_\rho(\tau_2, \tau_1) = \text{tr}(\phi^{(I)}(t(\tau_1), \mathbf{x}(\tau_1))\phi^{(I)}(t(\tau_2), \mathbf{x}(\tau_2))\rho). \quad (3)$$

This correlation function contains all the contribution of the field to first order in the photo-detecting signal. There is however a major difference between this signal and the standard one found by Glauber in quantum optics. Indeed, for photons, we have $G_\rho^{\text{ph}}(\tau_2, \tau_1) =$

$\text{tr}(E^-(\tau_2)E^+(\tau_1)\rho)$ where E^\pm are the positive and negative frequency parts of the electric field operator. In the relativistic regime, the correlation function does not only depend on the product $\phi^-\phi^+$ but on the full field as in Eq. (3) [21]. One reason behind this difference is fundamental and comes from the fact that the definition of positive and negative frequencies depends on the time coordinate. For a detector in a general trajectory or in the presence of a gravitational field, there is no global definition of time coordinate and so no general decomposition of the field in momentum space. The notion of excitation and of vacuum become relative concepts.

Equation (2) can be generalized by introducing a generic linear response function $\chi(\tau_2, \tau_1)$ of the detector and the resulting photo-detection signal is then obtained by

$$p(\tau) = \int_{\mathbb{R}} \chi_\tau(\tau_2, \tau_1) G(\tau_1, \tau_2) d\tau_1 d\tau_2. \quad (4)$$

The function $\chi_\tau(\tau_2, \tau_1)$ characterizes the response of the detector and its form depends on the type of detector we use. The photo-detection probability is then just the scalar product between this response function and the first order correlation function. For a broadband device, the response will be local in time with $\chi(\tau_2, \tau_1) = f(\tau)\delta(\tau_2 - \tau_1)$ and $f(\tau)$ the switching function. On the contrary, for a narrow-band device like the two-level system, we measure the Fourier transform of the correlation function.

B. Definitions

1. First-order and excess correlations

The photo-detection problem shows that the quantity encoding the response of point-like detector at first order, is given by a first-order correlation function of the field defined as:

$$G_\rho(\tau_2, \tau_1) = \text{tr}(\phi(\tau_1)\phi(\tau_2)\rho) = \langle \phi(\tau_1)\phi(\tau_2) \rangle_\rho \quad (5)$$

with the notation $\phi(\tau) = \phi^{(I)}(t(\tau), \mathbf{x}(\tau))$ for a given trajectory $x(\tau)$. Depending on the context, this function and all the higher-order ones that could be defined are called correlation functions or Wightman's functions. In quantum optics, the term coherence functions is used but involves correlation functions of the positive and negative frequency parts of the field. We will stick to general quantum field theory denomination of correlation functions. From now on, we use from now on a unit system in which $\hbar = c = 1$ and the Minkowski metric signature $(-, +, +, +)$.

The most important situation is when the vacuum state of the field is prepared. The correlation function

can be computed exactly and is given by:

$$G_{|0\rangle}(\tau_2, \tau_1) = \frac{1}{4\pi^2} \frac{1}{-(t(\tau_1) - t(\tau_2) + i\epsilon)^2 + (\mathbf{x}(\tau_1) - \mathbf{x}(\tau_2))^2}. \quad (6)$$

where, for the moment, we used the standard regularization of $i\epsilon$. The question of regularization will be discussed in more details in the next section.

Let's now add an extra-excitation in a normalized wave packet Φ :

$$\phi[\Phi] |0\rangle = \int_{\mathbb{R}^3} \Phi(t, \mathbf{x}) \phi^\dagger(t, \mathbf{x}) |0\rangle d^3x. \quad (7)$$

By Wick's theorem, and using the notation $\Phi^*(\mathbf{x}(\tau), t(\tau)) = \Phi(\tau)$, the first order correlation now reads:

$$G_{\phi[\Phi]|0\rangle}(\tau_2, \tau_1) = G_{|0\rangle}(\tau_2, \tau_1) + \Phi^*(\tau_1)\Phi(\tau_2) + \Phi(\tau_1)\Phi(\tau_2) + \text{h.c.} \quad (8)$$

This suggests to decompose the correlation function into two parts by the equation:

$$G_\rho(\tau_2, \tau_1) = G_{|0\rangle}(\tau_2, \tau_1) + \Delta G_\rho(\tau_2, \tau_1). \quad (9)$$

The interpretation is intuitively clear in the pure state case described by Eq. (8) since we can clearly think of excitations over the vacuum. For a general density matrix, the decomposition in Eq. (9) comes from the fact that a measurement must be understood as a comparison between the state of the field and a reference state, which in this case is the vacuum. This choice is also justified by the fact that a reasonable physical state will have the same behavior as the vacuum at high energy, both for absorption and emission processes. This turns out to be important for the regularization aspects, as we will see. However, such a decomposition might be more subtle when taking into account general relativity and backreaction effects.

In the following, Sec. III will focus on the vacuum contribution while the Sec. IV will be dedicated to the study of different kinds of excitation.

2. On regularization

In quantum field theory, the correlation functions are actually not proper functions but Lorentz-invariant distributions on spacetime [22]. The distribution character comes from the necessary divergences of the correlation functions which need to be properly regularized.

The standard $-i\epsilon$ regularization procedure, that was used for instance in Eq. (6), corresponds to an ultraviolet cut-off for the detector. However, in a general reference frame, the frequency content is redistributed and some care must be taken to ensure the proper regularization.

A natural choice is to do a high-energy cut-off regularization similar to the $-i\epsilon$ regularization of the modes in the proper reference frame of the detector [23].

This turns out to be equivalent to spatial regularizations, with spatially-extended detectors [5, 9, 24, 25], that were introduced to solve the issues encountered with causality leading to the impossibility to recover the Unruh effect with a causal detector [5], under the standard regularization scheme.

All those regularization procedure are equivalent and lead to a well defined Lorentz invariant and causal correlation functions. They amount to subtract the vacuum contribution found by an inertial detector [24]. In the end, this strategy matches the one used in quantum optics and condensed matter. The rationale behind it is physically intuitive, because the correlator itself is not probed directly, but always compared to the one of a reference state, as defined in Eq. (9).

C. Representations of the first order correlation

1. Time and frequency representations

The time representation $G_\rho(\tau_2, \tau_1)$ is the natural representation to look for dynamical information. The diagonal $G_\rho(\tau, \tau)$ corresponds to an energy density per unit time while the off-diagonal elements, which are complex numbers, give the coherences in time. However, this representation is not well suited to understand the kind of processes happening in the detection events since they are encoded in the $\tau_1 - \tau_2$ dependence of the phase of $G_\rho(\tau_2, \tau_1)$.

This is solved by going to the frequency domain. By computing a double Fourier transform, we can then define

$$G_\rho(\omega_2, \omega_1) = \int_{\mathbb{R}^2} G_\rho(\tau_2, \tau_1) e^{i(\omega_1\tau_1 - \omega_2\tau_2)} d\tau_1 d\tau_2 = \langle \phi^\dagger(\omega_1)\phi(\omega_2) \rangle_\rho \quad (10)$$

where the field $\phi(\omega)$ is defined with respect to an inertial mode decomposition as

$$\phi(\omega) = \int_{\mathbb{R}^3} \left(a_{\mathbf{k}} f_{\mathbf{k}}^*(\omega) + a_{\mathbf{k}}^\dagger f_{\mathbf{k}}(-\omega) \right) \frac{d^3\mathbf{k}}{2\omega_{\mathbf{k}}(2\pi)^3} \quad (11)$$

with

$$f_{\mathbf{k}}^*(\omega) = \int_{\mathbb{R}} e^{ik \cdot x(\tau)} e^{i\omega\tau} d\tau. \quad (12)$$

The Fourier plane (ω_1, ω_2) is traditionally divided into four quadrants as shown in Fig. 1. The positive frequency quadrant, defined by $\omega_1 > 0$ and $\omega_2 > 0$, corresponds to the absorption processes while the negative frequency quadrant corresponds to the emission processes. Finally, the two quadrants defined by $\omega_1\omega_2 < 0$ correspond to the coherences between emission and absorption processes. This interpretation follows the operational definition of particles and matches the many-body

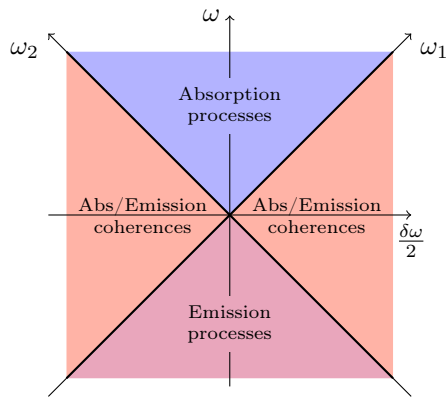


FIG. 1: Decomposition of the Fourier plane into four quadrants: the upper quadrant corresponds to absorption processes, the lower quadrant to emission processes and the side quadrants to the coherences between emission and absorption processes. While this particle-like interpretation makes sense for inertial observers, it does not necessarily hold as such for any trajectory.

one for inertial detectors. This equivalence does not hold for a general moving detector since nothing guarantees that the same notion of particles exists in all frames. Still we can expect that the different notions of particles that we could be defined should match at sufficiently high frequency (compared to acceleration or local curvature). This is corroborated for a uniformly accelerated detector: the inertial modes $u_\omega^{(a)}$ and the accelerated modes $u_\omega^{(i)}$ are related by a Bogoliubov transformation $u_\omega^{(a)} = (u_k^{(i)} - e^{-\pi\omega/a} \bar{u}_k^{(i)}) / \sqrt{1 - e^{-2\pi\omega/a}}$ from which we clearly see that for $\omega \gg a$, $u_\omega^{(a)} \approx u_k^{(i)}$. This remark suggests that instead of trying to define a global notion of particle, we should maybe seek to define local notions of particles relative to the different scales of the problem: this hints toward a time-frequency definition of particles, an idea that will be discussed in more details in Sec. V.

The diagonal $G_\rho(\omega, \omega)$ corresponds to the excitation occupation number per frequency. A convenient representation of the Fourier plane, also shown in Fig. 1, is given by the variables $\delta\omega = \omega_1 - \omega_2$ and $\omega = (\omega_1 + \omega_2)/2$ conjugated respectively to $\tau_1 - \tau_2$ and $(\tau_1 + \tau_2)/2$ which, as we will see, are the natural variables for the time-frequency Wigner representation.

The frequency domain representation has complementary advantages compared to the time representation. When analyzing the response of a detector in a stationary trajectory, choosing one representation over the other is a matter of convenience. However, most physically realizable motions are not stationary and a time-frequency representation is called for. Such representations exist and have been analyzed in depth in signal processing research [16]. The common one used in physics is the Wigner representation which we will discuss in the context of relativistic field theory.

2. Time-frequency representation

The time and frequency representations have complementary properties: while one clearly represents the time evolution, the other clearly shows the type of processes taking place. While this is not a major issue for stationary signals, it becomes one for non-stationary signal like those obtained by a detector moving in a general trajectory. Fortunately, it is possible to have the best of both worlds in one clear time-frequency representation. We propose to analyze the Wigner representation of the correlation function defined as:

$$W_\rho(\tau, \omega) = \int_{\mathbb{R}} G_\rho(\tau + v/2, \tau - v/2) e^{i\omega v} dv. \quad (13)$$

In the same way as Eq. (9), we can define an excess Wigner function ΔW_ρ with respect to the vacuum defined as:

$$W_\rho(\tau, \omega) = W_{|0\rangle}(\tau, \omega) + \Delta W_\rho(\tau, \omega). \quad (14)$$

The vacuum Wigner function must be regularized. As argued in Sec. II B 2, this is done by properly analyzing the response in the vacuum of an inertial detector and subtracting it. The Wigner function $W_{|0\rangle}$ is again decomposed into two contributions

$$W_{|0\rangle}(\tau, \omega) = W_{|0\rangle}^{\text{in}}(\tau, \omega) + \Delta_{\text{in}} W_{|0\rangle}(\tau, \omega). \quad (15)$$

The first one, $W_{|0\rangle}^{\text{in}}$, is the divergent inertial contribution which can be evaluated easily as $W_{|0\rangle}^{\text{in}} = \frac{|\omega|}{2\pi} \Theta(-\omega)$. The second, $\Delta_{\text{in}} W_{|0\rangle}$, is the regular part that encodes the non-inertial contributions. It is a Fourier transform of Eq. (6) (without the $i\epsilon$ regularization) defined by

$$\Delta_{\text{in}} W_{|0\rangle}(\tau, \omega) = \frac{1}{4\pi^2} \int_{\mathbb{R}} \left(\frac{1}{(\Delta x(\tau, v))^2} - \frac{1}{-\tau^2} \right) e^{i\omega v} dv \quad (16)$$

with $\Delta x(\tau, v) = x(\tau + v/2) - x(\tau - v/2)$.

The simplest situation is of course to consider an inertial detector in the vacuum. The response of the detector will then be given by $W(\tau, \omega) = \frac{|\omega|}{2\pi} \Theta(-\omega)$. This Wigner function is independent of τ which is a natural consequence of the stationary character of the trajectory. Its form could have been anticipated by remembering Fermi's Golden rule which states that the transition rate is given to first order by $2\pi d(\omega) f(\omega)$ with $d(\omega)$ the density of states and $f(\omega)$ the distribution both in energy space. For our relativistic set up, the relativistic density of state is given by $d^3 k / 2k^0 (2\pi)^3 = \omega d\omega / 4\pi^2$ since in the massless case $\omega = |\mathbf{k}|$.

Non-trivial physics is unraveled for a detector in a uniformly accelerated motion. Indeed, consider the trajectory to be $x(\tau) = (a^{-1} \sinh(a\tau), a^{-1}(\cosh(a\tau) - 1))$. Then the now well known thermal response is obtained:

$$\Delta_{\text{in}} W_{|0\rangle}(\tau, \omega) = \frac{\omega}{2\pi} \frac{1}{e^{2\pi\omega/a} - 1}. \quad (17)$$

While still stationary as expected, the Wigner function does not vanish for positive omega. This comes from the mixing of positive and negative frequencies between the inertial and uniformly accelerated modes. The response of the detector is the same as a thermal state with a temperature given by (using SI units)

$$T = \frac{\hbar}{ck_B} \frac{a}{2\pi}. \quad (18)$$

The Wigner function possesses a nice set of properties. First, for a stationary signal like the previous examples, the Wigner function is time independent and positive. Moreover, the Wigner function possesses a frequency symmetry $W(\tau, \omega) = W(\tau, -\omega)$ coming from the Hermitian property of the field. Second, its marginals give access to the probability distribution of the conjugated variable. For instance, averaging over time gives the spectral energy density distribution

$$f(\omega) = \overline{W(t, \omega)}^t. \quad (19)$$

In the T -periodic case, this average is taken over a time period, implying $f(\omega) = \frac{1}{T} \int_{-T/2}^{T/2} W(\tau, \omega) d\tau$. Similarly, the integration over frequency gives the power $P(\tau)$, which is finite only for the regularized Wigner function:

$$P(\tau) = \int \Delta_{\text{in}} W_\rho(\tau, \omega) \frac{d\omega}{2\pi} = \Delta_{\text{in}} G_\rho(\tau, \tau). \quad (20)$$

This quantity has an interesting relation to the trajectory of the detector in the one dimensional case as we will see later and it was proposed to use it as a general definition of temperature in curved spacetime [26, 27]. Finally, the average over time and positive frequency gives back the average energy measured by the detector

$$\langle E \rangle_\rho = \int_{\mathbb{R} \times [0, +\infty[} \Delta_{\text{in}} W_\rho(\tau, \omega) d\tau \frac{d\omega}{2\pi}, \quad (21)$$

an important property to keep in mind to normalize the states we will consider.

3. On causality

Many different kinds of time-frequency representations exist and have been analyzed in the signal processing literature [16]. They can be classified according to a set of natural properties we could demand for a good representation of physical processes: unitarity (a measurement result translates as a scalar product for representations), marginals corresponding to spectral density and power spectrum, positivity (negativities prevents probabilistic interpretations), linearity (a linear filter translates as a linear filter for the representations), causality and time-reversal symmetry. However, it happens that it is not possible to construct a function satisfying all those requirements. Table I shows the properties of two important time-frequency distributions.

Up to now, in the context of point-like detectors probing a relativistic quantum field, only the Page distribution, which is a causal time-frequency distribution, has been studied [5, 9, 24]. Indeed, the main motivation was to understand if the thermal behavior would appear in a causal response which is not how the standard Unruh effect is derived.

While this is more natural, the Page distribution is not convincingly more physical than a non-causal one since we still integrate over the whole past history of the motion. Indeed, a true physical response is causal and happens during a finite duration. This is properly modeled by considering a causal switching function $\chi_\tau(\tau_2, \tau_1)$ with finite support. By putting causality considerations in the switching function, focusing on the Page distribution is not mandatory anymore. It is even more interesting to consider the Wigner distribution, containing the same information as the Page one, since it has a clearer interpretation. First, time-reversal symmetry in the physical processes will be properly represented by the Wigner distribution. Moreover, the Wigner function possesses the linearity property which means that the Wigner transform of a linearly filtered signal is simply the scalar product between the Wigner functions of the filter and the original signal. This is a clear advantage over the other distribution for both signal processing tasks and interferometric experiments.

TABLE I: Comparison of the properties of the Page and Wigner distributions.

Properties	Wigner	Page
Unitarity	✓	✓
Positivity	✗	✗
Marginals	✓	✓
Linearity	✓	✗
Causality	✗	✓
Time reversal	✓	✗

III. A DETECTOR IN THE VACUUM

Let us now discuss the response of a detector probing the inertial vacuum. The main purpose here is to understand the structure of the Wigner function of the vacuum for a generic trajectory. After setting up the framework, we will first analyze the slow deviations from the uniformly accelerated case corresponding to the adiabatic approximation. We will then discuss its breakdown by analyzing oscillatory motions in the vacuum to finish with more physically realizable motions.

A. General 1+1D motion

To simplify the theoretical analysis, we will consider here a 1+1D generic motion. The solution of the special relativistic equations of motion for a detector can be parametrised in a transparent way. Starting from the normalization condition on the 4-velocity $-u_t^2 + u_x^2 = -1$, we have the natural parametrization:

$$\mathbf{u}(\tau) = \begin{pmatrix} \cosh A(\tau) \\ \sinh A(\tau) \end{pmatrix}. \quad (22)$$

By denoting $a(\tau)$ the oriented norm of the 4-acceleration $a^\mu(\tau)$ (positive if the acceleration goes towards $x > 0$, negative otherwise) and re-injecting into the equation for the 4-acceleration, we find that $a^2 = (\partial_\tau A)^2$ and, in the locally inertial frame at $\tau = 0$, we have

$$\mathbf{x}(\tau) = \begin{pmatrix} \int_0^\tau \cosh A(\tau') d\tau' \\ \int_0^\tau \sinh A(\tau') d\tau' \end{pmatrix} \quad (23)$$

where $A(\tau) = \int_0^\tau a(\tau') d\tau'$. From this we can go one step further and express $\Delta x^2(\tau + v/2, \tau - v/2)$ in a suitable form for analytical and numerical analysis. For that, we introduce the quantity:

$$A_\tau(v) = \int_\tau^{\tau+v} a(\tau') d\tau' = A(\tau + v) - A(\tau). \quad (24)$$

We then have:

$$\begin{aligned} \Delta x^2(\tau + v/2, \tau - v/2) = \\ - \int_{-\tau/2}^{\tau/2} \cosh(A_\tau(\tau_1) - A_\tau(\tau_2)) d\tau_1 d\tau_2. \end{aligned} \quad (25)$$

Using the cosh definition, we can see that this double integral can be re-expressed as a product of two simple ones:

$$\Delta x^2(\tau + v/2, \tau - v/2) = -f_+(\tau, v)f_-(\tau, v) \quad (26)$$

where $f_\pm(\tau, v) = \int_{-v/2}^{v/2} \exp(\pm A_\tau(v')) dv'$. We can also re-express the trajectory in terms of f_\pm . A description in the locally-inertial frame at time τ would simply be:

$$\Delta \mathbf{x}_\tau(v) = \frac{1}{2} \begin{pmatrix} f_+(\tau, v) + f_-(\tau, v) \\ f_+(\tau, v) - f_-(\tau, v) \end{pmatrix}. \quad (27)$$

This expression in terms of f_\pm possesses a few advantages. It is centered around τ , which allows to perform expansion for small values of v . Conversely, it allows precise numerical evaluation around small v values, which is of prime importance in the regularization scheme we have chosen.

The Wigner function can then be computed using Eq. (16). An interesting property can already be obtained for the power $P(\tau)$. Indeed, by computing the two sides of Eq. (20), we have:

$$P(\tau) = \frac{1}{4\pi^2} \frac{a_\tau^2}{12}. \quad (28)$$

The rationale behind defining local temperature in a general spacetime [26, 27] comes from this relation and the fact that the acceleration for a uniformly accelerated detector is proportional to the temperature (Eq. (18)), a property that remains true for an adiabatic motion as we will now see.

B. Adiabatic regime and its breakdown

1. Adiabatic regime

When acceleration changes slowly, we expect the Wigner function to be close to the uniformly accelerated case: this is called the adiabatic regime [7, 25, 28, 29]. More precisely, we expect that the main contribution to the Wigner function to be similar to a thermal response with a time dependent temperature $T(\tau)$ proportional to the instantaneous acceleration $a(\tau)$.

For the purpose of this discussion, we write explicitly the functional dependence on the acceleration of the Wigner function as $W[a(\tau)](\tau, \omega)$. Given a time τ , we denote the uniformly accelerated trajectory having the acceleration $a(\tau)$ by a_τ . Doing an expansion around this trajectory, we obtain

$$\begin{aligned} W[a(\tau)] = W[a_\tau] + \int_{\mathbb{R}} \frac{\delta W}{\delta a(v)} [a_\tau] \delta a(v) dv \\ + \frac{1}{2} \int_{\mathbb{R}^2} \frac{\delta^2 W}{\delta a(v_1) \delta a(v_2)} [a_\tau] \delta a(v_1) \delta a(v_2) dv_1 dv_2. \end{aligned} \quad (29)$$

The first term corresponds to the adiabatic response of the detector: the Wigner function is the thermal distribution with a time-dependent temperature proportional to the instantaneous acceleration a_τ . The other terms are corrections to this dominant term.

This development is meaningful when the variations of the acceleration $\delta a_\tau(v)$ around a given time τ are small compared to the acceleration a_τ over a timescale $\tau_s \gg a_\tau^{-1}$:

$$\delta a_\tau(v) \ll a_\tau \text{ with } v \leq \tau_s. \quad (30)$$

The timescale τ_s , that we could call adiabatic or stationary time, is of prime importance since it gives us the interval of time around τ over which we can consider the motion uniformly accelerated. Moreover, the variation $\delta a_\tau(v)$ can itself be seen as a function of the derivative $(\dot{a}, \ddot{a}, \dots)$. In good regimes, it is legitimate to do an expansion in those derivatives and obtain the reduced and more familiar criterion $\dot{a}/a^2 \ll 1$.

Thus both the amplitude and the frequency of the perturbation play a role in defining the adiabatic regime and deviations from it. To properly understand the different regimes of the response, we consider an oscillatory acceleration of the form $a(\tau) = a_0 + a_1 \sin(2\pi f\tau)$ with a_0 a constant acceleration and (a_1, f) the amplitude and frequency of the oscillatory drive [8]. The functional expansion of Eq. (29) can then qualitatively be seen as an

expansion in a_1/a_0 while the derivative expansion of δa is an expansion in $(2\pi f)/a_0$. The different regimes can then be classified as follows:

- The adiabatic regime is valid when the perturbation is small such that $a_1 \ll a_0$ and $2\pi f \ll a_0$. The thermal response follows the acceleration as in $W[a_\tau]$ and is corrected by small terms in the derivatives of the acceleration.
- The adiabatic regime *per se* breaks down when one of the two conditions above is not fulfilled and will be analyzed in the next section. In the regime $a_1 \ll a_0$ and $f \gtrsim a_0$, the functional expansion still works but the terms rearrange themselves such that a thermal response is still present at the average acceleration $\bar{a} = a_0$ plus corrections of order $1/f$.
- Finally, in the regime $a_1 \gtrsim a_0$, all the expansions break down and the structure of the Wigner function has to be analyzed differently.

We concentrate first on the pure adiabatic regime where we have $a_1 \ll a_0$ and $f \ll a_0$. In this regime, the intuition of a thermal response following the evolution of the acceleration works. Furthermore, the overall order of magnitude of a correction to $W[a_\tau]$ coming from the functional and derivative expansions is given by powers of the form $(2\pi f/a_0)^p \cdot (a_1/a_0)^q$. Table II sums this up from the first few corrections.

TABLE II: Orders of magnitude (in units of a_0) of the corrections in the functional and derivative expansion.

$O(\delta a)$	$O(\delta a^2)$	$O(\delta a^3)$
$(2\pi f)^2 a_1 [\ddot{a}]$	$(2\pi f)^2 a_1^2 [\dot{a}^2]$	–
–	$(2\pi f)^3 a_1^2 [\ddot{a}\dot{a}]$	$(2\pi f)^3 a_1^3 [\dot{a}^3]$
$(2\pi f)^4 a_1 [a^{(4)}]$	$(2\pi f)^4 a_1^2 [\ddot{a}^2]$	$(2\pi f)^4 a_1^3 [\dot{a}^2\dot{a}]$

Thanks to the symmetry of the Wigner function, the first correction in Eq. (29) only has even derivatives in a in the derivative expansion. This means in particular that there is no \dot{a} corrections to the thermal behavior. The first two corrections to the Wigner function have the following form:

$$W[a(\tau)] = W[a_\tau] + \frac{\ddot{a}}{a^2} \mathcal{P}_{12}[g](2\pi\omega/a_\tau) + \frac{\dot{a}^2}{a^3} \mathcal{P}_{22}[g](2\pi\omega/a_\tau) \quad (31)$$

where $g(x) = x/(e^x - 1)$ is the thermal distribution and the $\mathcal{P}_{ij} \in \mathbb{R}[Y, X]$ are polynomials of two variables such that the action on f is a derivative operation $\mathcal{P}_{ij}[g] \equiv \mathcal{P}_{ij}(x, \partial_x)[g(x)]$. Technical details about this derivation are given in Appendix B. Figure 2 represents the two functions $\mathcal{P}_{12}[g](x)$ and $\mathcal{P}_{22}[g](x)$ which are universal in the sense that they do not depend on the trajectory of the detector while Fig. 3 compares each correction to the

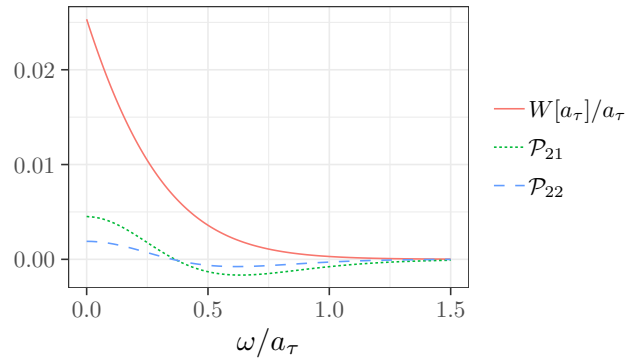


FIG. 2: Representation of the universal functions of the thermal distribution coming as corrections to the pure thermal response $W[a_\tau]$ in the derivative expansion. Their form is independent of the trajectory.

exact expression evaluated numerically at a given order. This shows that the corrections to the adiabatic thermal response are orders of magnitude less than $W[a_\tau]$, thus justifying that the regime $a_1 \ll a_0$ and $f \ll a_0$ corresponds indeed to an adiabatic regime where the thermal response follows the evolution of the acceleration.

2. Breakdown of the adiabatic regime

When the perturbation is too important, meaning that the conditions $a_1 \ll a_0$ and $f \ll a_0$ are not both fulfilled, the adiabatic response is not valid anymore. The simplest deviation we can first consider is $f \gtrsim a_0$. Intuitively, we expect that, since the frequency is too high, the thermal response cannot build up fast enough and follow the variations of the acceleration. Only an average thermal response at the acceleration \bar{a} should build up while traces of the oscillations should appear at higher frequencies in the time-frequency plane. This intuition can be explicitly checked by computing exactly the full first correction in Eq. (29) for the trajectory $a(\tau) = a_0 + a_1 \sin(2\pi f\tau)$ denoted $\Delta_0 W$. It actually contains all the derivative corrections $a^{(n)}$ of order n (first column of Table II). Its explicit form is given by

$$W_1 = \frac{a_1 \sin(2\pi f\tau)}{4\pi^2} \left[\frac{1}{1 + (2\pi f/a_\tau)^2} \frac{g_+ + g_-}{2} - \frac{\omega/2\pi f}{1 + (2\pi f/a_\tau)^2} (g_+ - g_-) + \frac{2\pi}{a_\tau} \omega \dot{g}_0 - g_0 \right] \quad (32)$$

where we reused $g(x)$ the thermal distribution and its values $g_\pm = g(2\pi/a(\omega \pm \pi f))$ and $g_0 = g(2\pi\omega/a)$. It can be explicitly checked that in the limit $f \ll a_0$, we recover the \ddot{a} correction to the adiabatic behavior.

From Eq. (32), we can now understand the high fre-

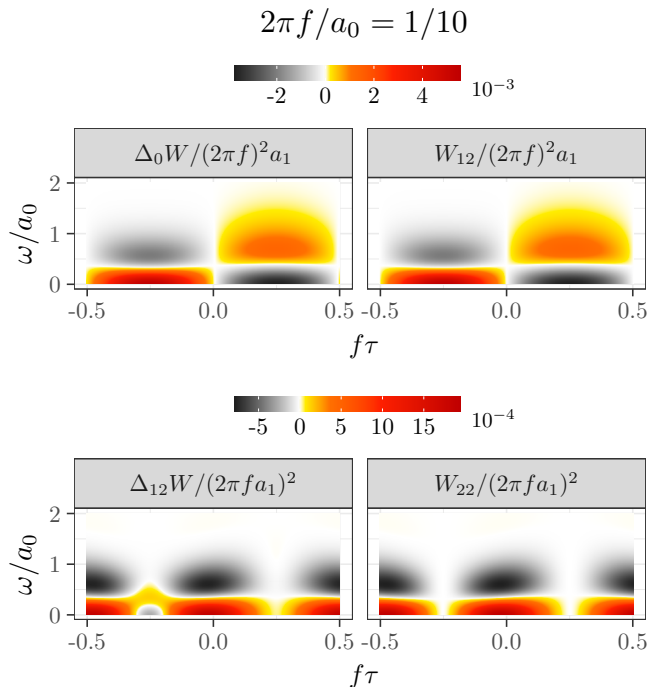


FIG. 3: Comparison between a correction to $W[a_\tau]$ at a given order W_{ij} and the exact one at the same order $\Delta_{ij}W = W - \sum_{(k,l) < (i,j)} W_{kl}$. In the adiabatic regime, at low frequency f , the derivative expansion is meaningful, each corrections being a order of magnitude lower than the previous one.

quency regime $f \gg a$. In the region $\omega \lesssim a_0$, we have

$$W_1 \approx \frac{a_1 \sin(2\pi f\tau)}{4\pi^2} \left[\frac{2\pi}{a_\tau} \omega \dot{g}_0 - g_0 \right]. \quad (33)$$

This expression has a nice interpretation: by considering a uniformly accelerated trajectory a_0 perturbed by a constant small term a_1 , we have $W[a_0 + a_1] = W[a_0] - \left[\frac{2\pi}{a_\tau} \omega \dot{g}_0 - g_0 \right] / 4\pi^2$. Thus, we conclude that in the region $\omega \lesssim a_0$ in the high-frequency regime the full Wigner function has the simple expression

$$W[a(\tau)] = W[\bar{a}]. \quad (34)$$

This matches the intuitive idea that the frequency of the perturbation is too high for a thermal behavior following the drive to build up. In fact, by a proper expansion of Eq. (32) in $2\pi f$ (done in Appendix B), we can see that there are corrections of order $1/2\pi f$ to the average thermal response in the frequency band $\omega \in [0, \pi f]$.

Finally, the expansion (29) breaks down completely when the criterion (30) is not satisfied. In the oscillatory example $a(\tau) = a_0 + a_1 \sin(2\pi f\tau)$, this qualitatively means that $a_1 \sim a_0$. In fact, this characterization is too brutal and global compared to the more local one from

Eq. (30): this means that globally the functional expansion cannot be performed but it can remain meaningful in some time intervals.

Figure 4 represents the Wigner function of the oscillatory acceleration for different parameters $(a_0/2\pi f, a_1/2\pi f)$. The global or local validity of the adiabatic expansion is witnessed by the appearance of inner oscillations in the Wigner function. In the regimes $(4, 1/4)$ and $(4, 1)$ for instance, the adiabatic expansion is globally valid. This is not anymore the case for the other regimes where $a_1 \sim a_0$ and where the signal basically goes (close) to zero at some moments in time. Still, the expansion remains meaningful locally half a period later. This can be made more quantitative by explicitly analyzing the criterion (30). As an example, consider the situation where $a_1 = a_0$. The criterion is then equivalent to $\cos(2\pi f\tau + \pi f v) \sin(\pi f v) \ll \cos^2(\pi/4 - \pi f t)$. Clearly, when $f\tau = -1/4$, the criterion cannot be satisfied and the adiabatic expansion breaks down while it is valid around $f\tau = 1/4$ (see Fig. 4). How can this be interpreted will be discussed in more details in Sec. V.

3. A more physical trajectory

The previous analyses, while important in their own regard to understand how the response changes in non stationary situations, are still based on non physical trajectories since they require an infinite amount of energy to be sustained. The question then remains on understanding the form of the Wigner function for physical trajectories [25, 30, 31].

Figure 5 represents the Wigner function (left panel) of a trajectory uniformly accelerated for a finite duration $a\tau = 4$. To make contact with the literature, it also shows (right panel) the Page distribution for the same trajectory. Besides the obvious causal response, we can see that a thermal response is building up over a timescale of a few a . It is to be noted that the Page distribution, like the Wigner function, is not always positive in the time-frequency plane.

Concerning the Wigner function, its general features can be well understood. First, we see that a thermal response at temperature $a/2\pi$ appears over a timescale of the order of a . Second, the high-frequency structure around the beginning of the accelerated phase depends solely on the discontinuity in the acceleration. In our case of interest, we expect the second and higher derivatives of the first order correlation to be discontinuous. To analyze their effects on the Wigner representation, it is useful to use the following decomposition $G(\tau + v/2, \tau - v/2) = f_\tau(v) + g_\tau(v)$ where f contains the lower order discontinuity contribution and g the higher order ones. The detailed form of those functions are irrelevant for the high-frequency behavior and can be chosen for computational convenience: the only constraints are that should capture the form of the discontinuities (see Appendix A for details on this strategy). In the end, we

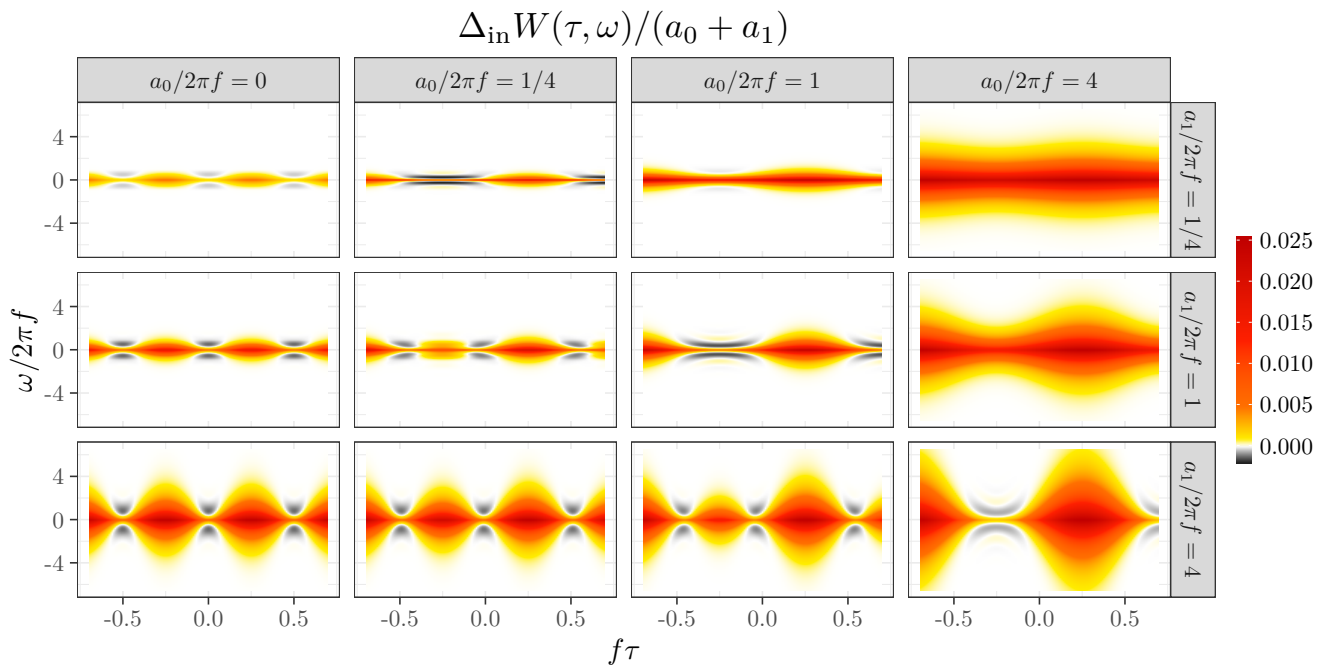


FIG. 4: Wigner function representation of an oscillatory acceleration $a(\tau) = a_0 + a_1 \sin(2\pi f\tau)$ in different regimes controlled by the expansion parameters $(a_0/2\pi f)$ and (a_1/a_0) . In the regime of small frequency f and amplitude a_1 compared to a_0 , the adiabatic response works globally. Outside this regime, the adiabatic expansion breaks down, which is witnessed by the appearance of inner oscillations, but can still be meaningful locally.

obtain the high frequency behavior of the Wigner function around the times τ_d of brutal discontinuous changes of the acceleration as:

$$\Delta W(\tau \geq \tau_d, \omega) \simeq -\frac{1}{4\pi^2} \frac{a}{8 \sinh^2 a(\tau - \tau_d)} \frac{\sin 2\omega(\tau - \tau_d)}{(\omega/a)^3} \quad (35a)$$

$$\Delta W(\tau \leq \tau_d, \omega) \simeq -\frac{1}{4\pi^2} \frac{a}{16a^3(\tau - \tau_d)^3} \frac{\cos 2\omega(\tau - \tau_d)}{(\omega/a)^4} \quad (35b)$$

IV. EXCESS CORRELATION FOR DIFFERENT TRAJECTORIES

Up to now, we have only been interested in the first order correlation of the vacuum. We now move to the subject of the excitations above the vacuum and how they are perceived by a moving detector [32]. From Eq. (8), the excess correlation coming from a one-particle excitation in a wavefunction $\Phi(t, \mathbf{x})$ is given by

$$\Delta G_\rho(\tau_2, \tau_1) = \Phi^*(\tau_1)\Phi(\tau_2) + \Phi(\tau_1)\Phi(\tau_2) + \text{h.c.} \quad (36)$$

The nice feature of this correlation function is that its form is independent of the trajectory of the detector which is a direct consequence of the covariance properties of the quantum field correlation functions.

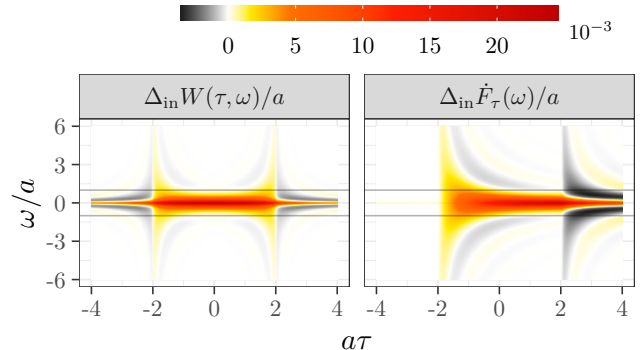


FIG. 5: Wigner (left) and Page (right) distributions of the vacuum for a finite duration uniform acceleration between two inertial phases. After a transition time of the order of a^{-1} , the thermal behavior at temperature $a/2\pi$ settles down. The decreasing oscillating high-frequency parts are solely controlled by the discontinuity of the acceleration.

The states mostly considered in a quantum optics setting are Fock states and coherent states. The main difference between the two in the first order correlation is the absence (resp. presence) of the interference terms $\Phi(\tau_1)\Phi(\tau_2) + \text{h.c.}$ for Fock states (resp. coherent states).

Finally, those states can be prepared in different wavepackets like a monochromatic one or a Gaussian

one. In what follows, we will mainly focus on Gaussian wavepackets of coherent and Fock states, which are in the end the most intuitive ones. We leave the mathematical analysis of the monochromatic case for Appendix C.

A. Gaussian wavepacket

Let us consider, for now in 3+1D, that the inertial observer prepares the field in a Gaussian coherent state. It is defined in the following way:

$$|\alpha\rangle = \bigotimes_{\mathbf{p}} |\alpha_{\mathbf{p}}\rangle = e^{\int_{\mathbb{R}^3} (\alpha_{\mathbf{p}} a_{\mathbf{p}}^\dagger - \alpha_{\mathbf{p}}^* a_{\mathbf{p}}) d^3p} |0\rangle. \quad (37)$$

The exponential operator is called the displacement operator $D(\alpha)$. This state is normalized and satisfies the fundamental relations of coherent states¹

$$D(-\alpha) a_{\mathbf{p}} D(\alpha) = a_{\mathbf{p}} + (2\pi)^3 2\omega_{\mathbf{p}} \alpha_{\mathbf{p}}, \quad (38a)$$

$$a_{\mathbf{p}} |\alpha\rangle = (2\pi)^3 2\omega_{\mathbf{p}} \alpha_{\mathbf{p}} |\alpha\rangle. \quad (38b)$$

We can also think of this state in a spatial way by looking at its action on a field operator. Indeed,

$$D(-\alpha) \phi^+(x, t) D(\alpha) = \phi^+(x, t) + \Phi_{\alpha}(x, t). \quad (39)$$

where ϕ^+ is the negative frequency part of the field. Thus we see that the state (37) is a coherent state in position with a parameter given by

$$\Phi_{\alpha}(x, t) = \int_{\mathbb{R}^3} \alpha_{\mathbf{p}} e^{-i(\omega_{\mathbf{p}} t - \mathbf{p} \cdot \mathbf{x})} d^3p. \quad (40)$$

We see that at $t = 0$ it is just the Fourier transform of the coherent state parameter in momentum space. From the factorized nature of this state, the first order correlation function can be decomposed into clear different contributions

$$\begin{aligned} \Delta G_{|\alpha\rangle}(\tau_2, \tau_1) &= \Phi_{\alpha}(\tau_1) \Phi_{\alpha}(\tau_2) + \Phi_{\alpha}(\tau_1) \Phi_{\alpha}^*(\tau_2) \\ &+ \text{h.c.} \end{aligned} \quad (41)$$

We now specify the function $\alpha_{\mathbf{p}}$ and choose it so that the problem reduces effectively to a 1+1D problem for computational simplicity. We then consider a Gaussian centered at a given momentum p_0 , with a width given by σ_p . We then have

$$\alpha_p = \sqrt{\frac{p_0}{2\pi}} \frac{1}{(2\pi\sigma_p^2)^{1/4}} e^{-\frac{(p-p_0)^2}{4\sigma_p^2}} e^{-ip \cdot x_0}. \quad (42)$$

In position it is a Gaussian centered at the position x_0 . We also make the following assumption that $p_0 \gg \sigma_p$

so that we can make consider that $\omega_p = |p| = p$ in our computations. This leads to

$$\Phi_{\alpha}(\tau) = \sqrt{\frac{p_0}{(2\pi\sigma_x^2)^{1/2}}} e^{-[(t_{\tau} - x_{\tau}) + x_0]^2 / 4\sigma_x^2} e^{-ip_0[(t_{\tau} - x_{\tau}) + x_0]}. \quad (43)$$

The introduction of the normalization $\sqrt{p_0/2\pi}$ comes from dimensional considerations since we require the average energy to equal the average value of the Wigner function over time and frequency (see Eq. (21)). We also introduced the position width σ_x satisfying the relation $\sigma_x \sigma_p = 1/2$.

As an example, consider an inertial trajectory with a velocity v , the world-line is parametrized as $(\gamma\tau, \gamma v\tau)$. Its Wigner function is:

$$\begin{aligned} W^{(v)}(\tau, \omega) &= 2p_0 \left[e^{-\frac{(\omega - D_v p_0)^2}{2(D_v \sigma_p)^2}} + e^{-\frac{(\omega + D_v p_0)^2}{2(D_v \sigma_p)^2}} + \right. \\ &\left. 2 \cos(2p_0(D_v \tau + x_0)) e^{-\frac{\omega^2}{2(D_v \sigma_p)^2}} \right] e^{-\frac{(D_v \tau + x_0)^2}{2\sigma_x^2}}. \end{aligned} \quad (44)$$

The computation is straightforward and the Wigner function is composed of two symmetric Gaussian spots centered around the Doppler shifted frequency $D_v p_0$ with their interference pattern.

Gaussian spots are in fact the basic ‘‘atoms’’ of the Wigner function and allow to understand the geometry behind this representation [16]. The basic interpretative element that we need and that we see in Eq. (44) is that the interference term of two Gaussian atoms is also a Gaussian spot located at the mid-point joining the center of the two atoms (here $\omega = 0$) and that the interference pattern oscillates in the orthogonal direction.

This discussion would be completely similar if, instead of Gaussian coherent states, we consider a Gaussian superposition of a Fock state of n photons. The excess correlation is even simpler since the interference terms vanish: $\Delta G_{|n_{\alpha}\rangle} = n \Phi_{n_{\alpha}}^* \Phi_{n_{\alpha}} + \text{h.c.}$

While those Wigner functions could have been guessed intuitively for an inertial response, it is a non-trivial task to analyze the response to a Gaussian excitation from a moving detector for different accelerated trajectories.

B. Accelerated Wigner function

1. Uniformly accelerated case

Suppose now that the Gaussian coherent state, prepared by the inertial observer, is probed by a uniformly accelerated detector following the worldline $(a^{-1} \sinh a\tau, a^{-1}(\cosh a\tau - 1))$ in 1+1D. Figure 6 shows both the Wigner function of a Fock and coherent Gaussian states evaluated numerically. Each snapshot represents the Wigner function for a pulse emitted at a different position x_0 . As the intuition would suggest, the

¹ This is obtained from the BCH formula and the covariant commutation relations $[a_{\mathbf{p}}, a_{\mathbf{p}'}^\dagger] = (2\pi)^3 2\omega_{\mathbf{p}} \delta(\mathbf{p} - \mathbf{p}')$.

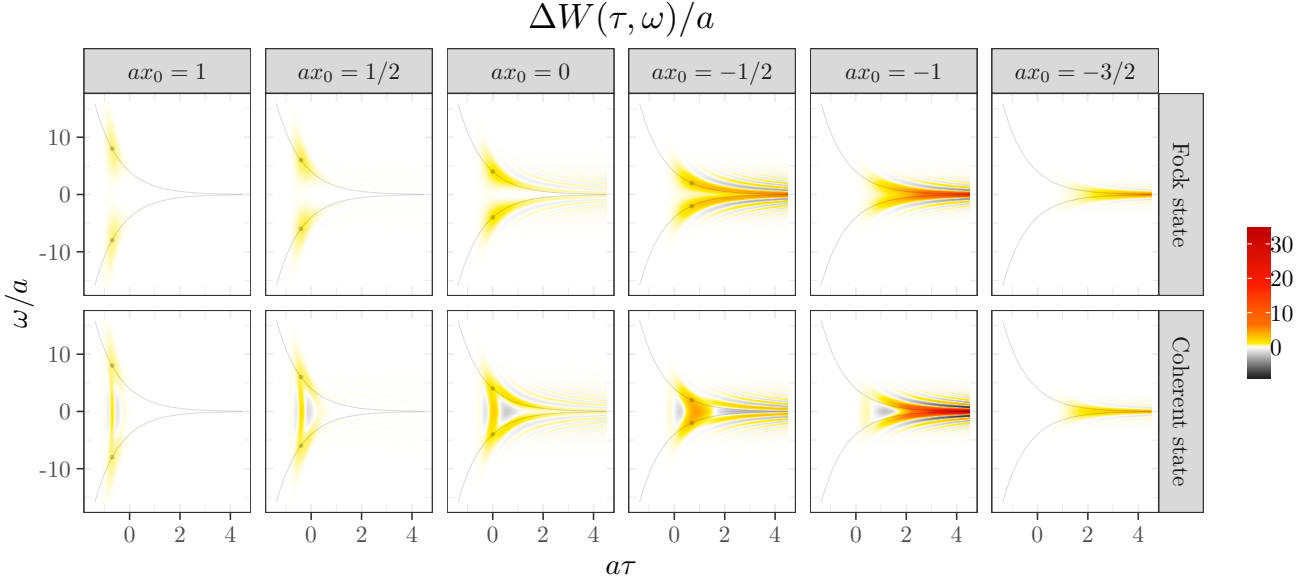


FIG. 6: Evolution of the Wigner function of Gaussian Fock state (top row) and coherent state (bottom row) emitted at different positions x_0 , with a frequency $p_0/a = 4$ and a width $a\sigma_x = 1/2$ in the inertial frame. The signal is centered around a spot at (τ_r, ω_r) given by Eqs. (45) and (47) which are respectively the special relativistic reception time and frequency and follows the instantaneous frequency curve for different x_0 . As the emission gets closer to the horizon, the spot flattens and gets strongly redshifted.

closer the emission is to the horizon the more redshifted and deformed the wavepacket is.

A closed analytical form cannot be obtained in this case but the structure of the Wigner function can be completely understood using Gaussian and stationary phase approximation schemes and its first correction. The detailed treatment is given in Appendix D. For clarity, let's focus on the $\Phi_\alpha(t, x)\Phi_\alpha^*(t', x')$ contribution of the Wigner obtained from Eq. (43) evaluated on the uniformly accelerated trajectory.

The first approximation scheme that we can employ is to approximate the received wavepacket by a Gaussian function around its maximum reached at time τ_r . Physically, this is the time of reception for the moving detector. It is obtained by solving $t_\tau - x_\tau + x_0 = 0$ which gives the special relativistic result:

$$\tau_r = -a^{-1} \ln(1 + ax_0). \quad (45)$$

Computing the Wigner function is then straightforward and gives

$$W_{\Phi_\alpha \Phi_\alpha^*}(\tau, \omega) = \frac{2p_0}{D_r} \exp\left(-\frac{D_r^2}{2\sigma_x^2}(\tau - \tau_r)^2\right) \exp\left(-\frac{1}{2} \frac{4\sigma_x^2}{D_r^2} (\omega - \omega_r(1 - a(\tau - \tau_r)))^2\right) \quad (46)$$

with $D_r = e^{-a\tau_r}$ the "gravitational" redshift and ω_r the shifted frequency measured by the moving detector,

$$\omega_r = p_0 e^{-a\tau_r} = p_0(1 + ax_0). \quad (47)$$

This is the uniformly accelerated analogue of the Einstein effect. Thus, we recover directly at this level of approximation the standard results of light perceived by a uniformly accelerated observer in a special relativistic setting.

While this rough Gaussian approximation allows us to pinpoint the dominant part of the Wigner function in the time-frequency plane, it is not well suited to understand the inner interference pattern. However, the stationary phase approximation scheme can. Writing the Wigner function as $W_{\Phi_\alpha \Phi_\alpha^*}(\tau, \omega) = \int_{\mathbb{R}} A(v; \tau) e^{i\Phi(v; \tau, \omega)} dv$, the stationary phase is meaningful when the velocity of phase oscillations is larger than the variations of the modulus. This is indeed the case here since the phase blows up exponentially compared to the Gaussian decay of the modulus. Now, we have to find the stationary points and compute the derivatives at those points. The stationary points τ_s are solutions of:

$$\frac{\partial \Phi}{\partial v}(\tau_s; \tau, \omega) = 0 \Rightarrow \begin{cases} \frac{\omega}{p_0} e^{a\tau} = \cosh a\tau_s/2, & \frac{\omega}{p_0} e^{a\tau} \geq 1 \\ \emptyset & \text{otherwise} \end{cases}. \quad (48)$$

We have two symmetric solutions τ_s and $-\tau_s$. The condition of existence shows that the stationary phase approximation is defined in the convex hull of the instantaneous frequency curve $\omega(\tau) = p_0 e^{-a\tau}$. The second derivative evaluated at τ_s gives the validity domain of the stationary

phase approximation. On the positive solution τ_s :

$$\begin{aligned} \frac{\partial^2 \Phi}{\partial v^2}(\tau_s; \tau, \omega) &= -\frac{a}{2} \omega(\tau) \sinh \left(\operatorname{arcosh} \left(\frac{\omega}{\omega(\tau)} \right) \right) \\ \Rightarrow_{\tau_s > 0} \frac{\partial^2 \Phi}{\partial v^2}(\tau_s; \tau, \omega) &= -\frac{a}{2} \sqrt{\omega^2 - \omega^2(\tau)} \leq 0. \end{aligned} \quad (49)$$

Away from the instantaneous curve and inside its convex hull, the Wigner function is well approximated by the stationary phase approximation. Its explicit derivation is given in Appendix D and we have:

$$\begin{aligned} W_{\Phi_\alpha \Phi_\alpha^*}(\tau, \omega) &= \sqrt{\frac{8p_0^2}{a\sigma_x^2} \frac{\exp \left(-\frac{(\omega - \omega_r)^2 + [\omega - \omega(t)][\omega + \omega(t)]}{2(ap_0\sigma_x)^2} \right)}{\sqrt{\omega^2 - \omega^2(t)}}} \\ &\quad \cos \left(2 \left[\frac{1 - \ln 2}{a} - \tau \right] \omega + \frac{\pi}{4} \right). \end{aligned} \quad (50)$$

This form can be interpreted as follows. First, oscillations are present in the Wigner function, given by the cosine term, covering the whole time-frequency plane. Second, the dominant contribution is at the intersection of a strip centered around the frequency ω_r and a tube following the instantaneous frequency $\omega(t)$. This allows to understand pictorially why interferences appear as we get closer to the horizon: the intersection region gets wider as we get closer, allowing the interferences to be visible.

To be rigorous, the approximation fails on the instantaneous curve $\omega(\tau)$. We should then go to the next order of approximation: this is the Airy approximation. Fortunately, since $\frac{\partial^3 \Phi}{\partial \tau^3}(\tau_s; \tau, \omega(\tau)) \neq 0$, we do not need to go to a higher order. The behavior of the Airy function is controlled by the curvature $\epsilon(\tau)$ of the instantaneous frequency:

$$\epsilon(\tau) = \frac{1}{4\pi} \left(\frac{d^2 \omega(\tau)}{dt^2} \right)^{1/3} = \frac{(a^2 \omega(\tau))^{1/3}}{4\pi}. \quad (51)$$

Nonetheless, the stationary phase approximation (and its corrections) of the Wigner function gives already the general qualitative structure of the oscillations that we can see on Fig. 6.

2. General 1 + 1 d trajectory

For a generic trajectory, it is of course not possible to obtain a complete analytical form of the Wigner function. Nonetheless, its general features are clearly obtained from the Gaussian and stationary phase approximations that we already used for the uniformly accelerated case. Indeed, from the detailed computations presented in Appendix D, we can prove the intuitive idea that first the Gaussian spot is shifted in the time-frequency plane by the "gravitational" redshift. The instantaneous frequency curve that the spot is following is given by (see Sec. III A

for the notations):

$$\omega(\tau) = p_0 e^{-A(\tau)} \quad \text{with} \quad A(\tau) = \int_0^\tau a(u) du. \quad (52)$$

The spot is centered around the reception time τ_r which is a solution of the equation $\int_0^{\tau_r} \exp(-A(u)) du = -x_0$. Since the term in the integrand is positive, this equation possesses either no or a single solution. This comes from the fact that the observer necessarily travels slower than the speed of light. As such it is only possible to meet the photon once. If this equation has no solution, it means that the photon was emitted behind the event horizon of the observer. We note that, at this order of approximation, the chirp rate is what we classically expect: it is given by the variation of the frequency shift for different times which is here $\frac{d\omega(\tau)}{d\tau} = -a(\tau)\omega(\tau)$.

The inner interference pattern (inside the convex hull defined by the instantaneous frequency curve) is once again understood by resorting to the stationary phase approximation and its Airy correction.

Figure 7 shows the response of a moving detector following a uniformly accelerated by parts trajectory. Starting from inertial motion, the first phase of the motion accelerates uniformly with acceleration a at time $a\tau = -2$ up until time $a\tau = -1$. The second phase between $a\tau = -1$ and $a\tau = 1$ has acceleration $-a$. The last phase has again acceleration a up until $a\tau = 2$ with inertial motion onward. This is the kind of trajectory considered in the twin paradox setup. The signal follows the instantaneous frequency curve which can be computed exactly in this case and the wavepacket is deformed, chirped, along it.

C. Transformation of coherence

The mathematical framework developed so far is also well suited to analyze superpositions. Let's again consider a one particle excitation which is now prepared in a wavepacket $\Phi(x)$ composed of a linear combination of elementary ones $\Phi_k(x)$ as:

$$\Phi(x) = \sum_k a_k \Phi_k(x). \quad (53)$$

In this case, it is straightforward to show that:

$$\Delta W(\tau, \omega) = \sum_{k, k'} a_{k'}^* a_k \Delta W_{kk'}(\tau, \omega) \quad (54)$$

where we introduced the notation

$$\Delta W_{kk'}(\tau, \omega) = \int_{\mathbb{R}} \Phi_{k'}^*(\tau - v/2) \Phi_k(\tau + v/2) e^{i\omega v} dv. \quad (55)$$

When $k = k'$, we recognize that $\Delta W_{kk'}$ is the excess Wigner function in the presence of the excitation Φ_k . Furthermore, $k \neq k'$ indicates cross terms, responsible for the so-called outer interference terms, between the

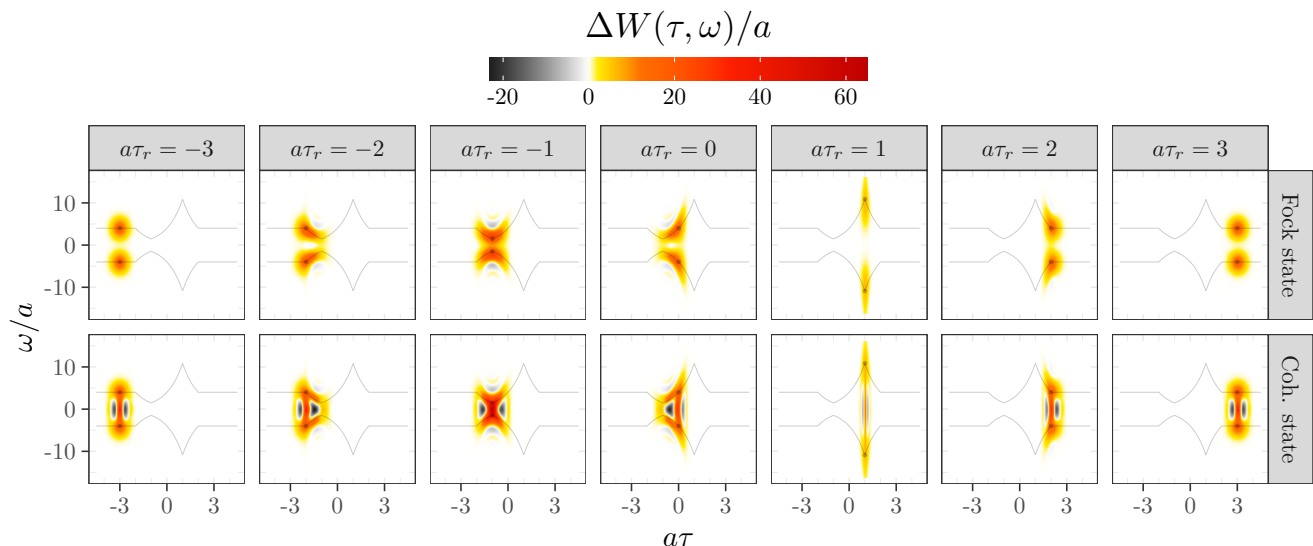


FIG. 7: Wigner function representations of a Gaussian Fock state (top row) and Gaussian coherent state (bottom row) probed by a detector following a uniformly accelerated twin-like trajectory: the spot is chirped by the accelerated motion with a rate $-a(\tau)\omega(\tau)$ but follows the instantaneous frequency curve. The total time of the accelerating phase is $a\tau_{\text{acc}} = 4$, with transitions at $\tau = -2, -1, 1, 2$. The frequency of the wavepacket in the inertial frame is $p_0/a = 4$ and its width is $a\sigma_x = 1/3$.

different components Φ_k . Those interferences were already present in Figs. 6 and 7 for the Gaussian coherent state. The total excess Wigner function can thus be expressed as a sum containing the main components and cross-terms:

$$\begin{aligned} \Delta W(\tau, \omega) &= \sum_k |a_k|^2 \Delta W_{kk}(\tau, \omega) \\ &+ \sum_{k \neq k'} a_{k'}^* a_k \Delta W_{kk'}(\tau, \omega). \end{aligned} \quad (56)$$

The important message here is that the excess terms deform naturally. If we start with some spatial superposition, each term will be deformed as if it were alone. At the same time, the outer interference terms depends only on the deformed wavepackets. This means that if we emit a wavepacket in a linear superposition of two wavepackets received around times τ_1 and τ_2 , we expect that the interference terms will be located at the midpoint $\tau_m = (\tau_1 + \tau_2)/2$. Furthermore, those interference terms will not depend on the details of the trajectory at time τ_m but on those at the times of reception τ_1 and τ_2 .

Figure 8 considers once again the uniformly accelerated twin-like trajectory of Sec. IV B 2. The field is however prepared in a spatial superposition of two Gaussian wavepackets (only the photon wavefunction is represented for clarity):

$$\Phi(x) = \Phi_2(x) + \Phi_1(x) \quad (57)$$

where the wavepacket $\Phi_i(x)$ is centered around the position x_i and is received by an inertial observer at time t_{r_i} and by the moving detector at times τ_{r_i} . Quite naturally, the structure of the Wigner function depends on

the spatial separation of the components of the superposition or, equivalently, on the detection times, and the local characteristics of the trajectory.

First, by denoting $\mathcal{J}^-(x)$ the causal past of a point x in spacetime, the coherence properties are modified by the motion of the detector only if at least one component has been prepared in the spacetime region $\mathcal{J}^-(f) \setminus \mathcal{J}^-(i)$ where i and f are respectively the beginning and end events of the acceleration phase.

The second feature concerns the delay time between the reception of the two wavepackets. On Fig. 8, the wavepackets were prepared such that the inertial delay $\Delta t_r = 4a^{-1} \sinh(a\Delta\tau_r/4)$ with $\Delta\tau_r = 3$ which is the general twin-paradox delay formula for this trajectory. This time-delay is clearly seen in the Wigner function and satisfies the special relativistic result (Fig. 12 compares the inertial and accelerated responses directly).

Finally, while the coherence pattern is identical to a pure inertial response when the packets are prepared outside the region $\mathcal{J}^-(f) \setminus \mathcal{J}^-(i)$, the interference pattern is clearly deformed by the motion of the detector when one component is probed in the accelerated phase.

Figure 9 shows the more extreme case of the evolution of coherence of a Gaussian superposition probed by a uniformly accelerated detector. The spacetime geometry probed by this detector, also called Rindler spacetime or wedge, is quite different than the previous case because of the presence of an event horizon. Naturally, a detection event occurs if and only if the wavefunction has been prepared with a support in the wedge. The situation shown in Fig. 9 represents a Gaussian superposition of two wavepackets, one of which propagates closer and closer to the horizon. The coherence gets spread and red-

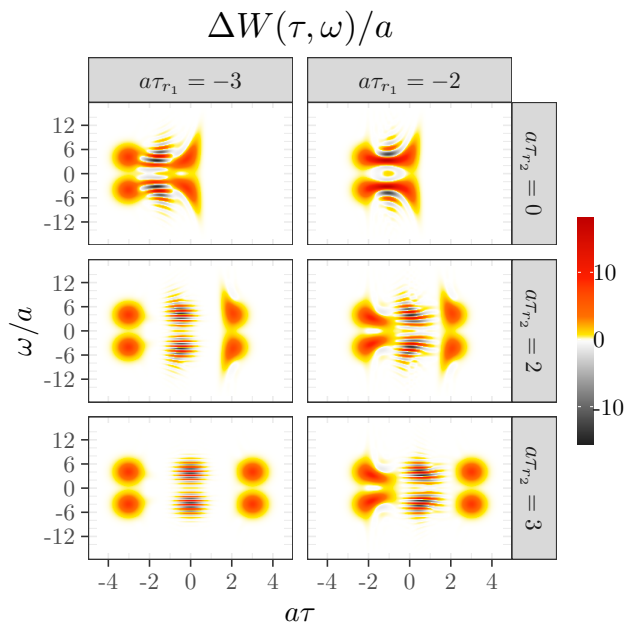


FIG. 8: Wigner function representation of a superposition of a Gaussian photon wavepacket probed by a detector following a uniformly accelerated twin-like trajectory for different $\tau_{r,1}$ and $\tau_{r,2}$ reception times respectively associated to the first and second component of the superposition. The total time of the accelerating phase is $a\tau_{\text{acc}} = 4$ with transitions at $\tau = -2, -1, 1, 2$. The wavepacket is emitted at frequency $p_0/a = 4$ in the inertial frame with a width $a\sigma_x = 1/3$.

shited as the wavepacket approaches the horizon which is a consequence of the same effects happening to the wavepacket itself.

After crossing the horizon, no detection signals can be recovered by the detector and the coherences are lost. This is of course the same effect happening in black hole physics which leads to the famous information paradox. We should note that this loss of coherence cannot be properly qualified as a decoherence process in the traditional sense where an environment interacts with the system and attenuates the interference pattern. Indeed, the deformation and loss of coherence only comes about because the wavepacket themselves are deformed by motion or lost behind an horizon which is not what decoherence is about.

V. DISCUSSIONS

So far, the point of view we adopted was a pure signal processing one. Indeed, our interest was only focused on doing a proper analysis of signals characterized by correlation functions $G_\rho(\tau_1, \dots, \tau_n)$ obtained from a set of point-like detectors. The question remains on how to relate those signals to quantum field theories for different observers [6, 33, 34].

The fundamental question at this stage is to under-

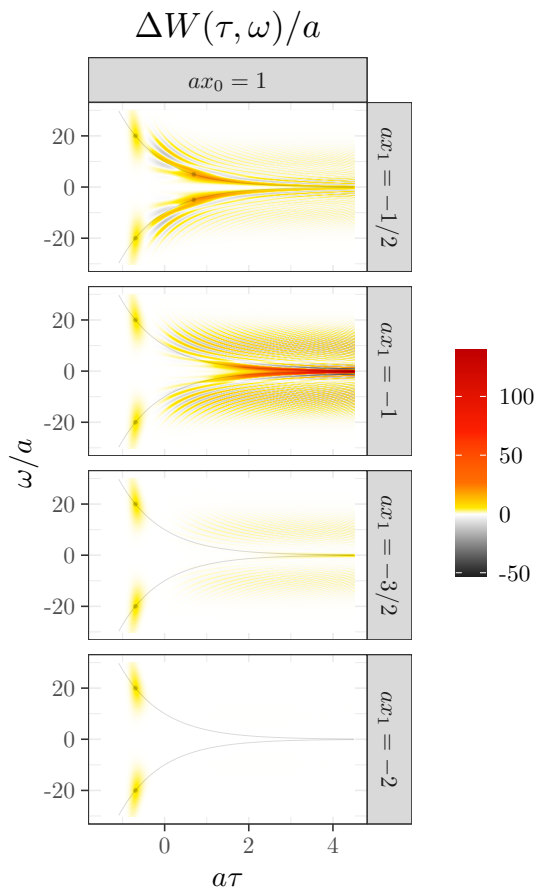


FIG. 9: Wigner function representations of a Gaussian superposition received at different times for a uniformly accelerated observer. The coherences are spread and eventually lost when a member of the superposition gets close or cross the horizon. The wavepacket is emitted at frequency $p_0/a = 10$ in the inertial frame with a width $a\sigma_x = 1/5$.

stand what can be reconstructed about the quantum field from the signals (of one or a set of detectors). To be more precise, we can roughly group the questions in two categories:

- What can we learn about the trajectory of the detector with respect to laboratory frame θ ?
- Can we reconstruct a field theoretic picture $(\mathcal{H}_\theta, f_\theta)$ from the signals, with \mathcal{H}_θ the Hilbert space of the theory and f_θ the mode on which the field is decomposed?

Our signal processing approach opens up some interesting perspectives on those questions.

Concerning the recovery of information about the trajectory, we need a prior information about what was sent by the laboratory. Indeed, it is conceivable to imagine only inertial detectors probing a state prepared in such a way as to simulate an accelerated response. So to not be fooled by what we measure, we need, for instance, the

laboratory to communicate to the accelerated observer what they originally prepared. Information about the trajectory can then be recovered by properly fitting the measured signal or, if we have enough data, reconstruct the instantaneous frequency curve from which the acceleration can be deduce since $d\omega(\tau)/d\tau = -a(\tau)\omega(\tau)$. If no excitations are present, we can still have some information about the trajectory from the power spectrum Eq. (28) of the vacuum: indeed, for a one dimensional motion, it is directly proportional to the square of the acceleration.

The second question was about reconstructing a field theoretic or many-body point of view from the signals. While we are not going to investigate thoroughly this complicated question, time-frequency analysis can shed some light on one particular issue concerning the definition of a notion of particles.

In the standard many-body approach, there is no issue to define a notion of particles in a stationary situation [35] like a uniformly accelerated motion. Qualitatively, we have a notion of time from which we can define a Fourier transform. There is however no general method to define a notion of particles in non-stationary situations. In other words, the notion of particles is an emerging notion [36]. It is nonetheless interesting to link this emerging notion to the notion encountered in the standard many-body approach.

One way to do this is to introduce an operational notion of particles thanks to response signals $G(\tau_1, \tau_2)$ of detectors [4]. The question is to then relate those two notions which, in general, are quite different. As we already mentioned, it is valid to interpret $G_\rho(\omega, \omega')$ in terms of excitations for inertial detectors as is usually done, for instance, in quantum optics: the two notions coincide. This breaks down *a priori* in non-stationary motions.

The time-frequency analysis of the complete signal offers a strategy to link the two notions and reconstruct a many-body particle interpretation. Indeed, from the full signal, it is possible to extract stationary domains [37]. Intuitively speaking, we can extract domains where it is meaningful to decompose the field modes like $f_{\mathbf{p}}(\tau, \mathbf{r}) \propto e^{-i\omega_{\mathbf{p}}\tau} f_{\mathbf{p}}(\mathbf{r})$ [6]. Knowing then the stationary time scales and averaging the signal over them, notions of particles could then be locally defined. Operationally speaking, what can be done is to consider a detector with a response function having support on those domains.

To illustrate this strategy, let's consider again the situation studied in Sec. III B where we considered an oscillatory motion of the form $a(\tau) = a_0 + a_1 \sin(2\pi f\tau)$ represented in Fig. 4. This situation is completely non stationary and even not globally adiabatic when $a_0 = a_1$. No natural particle interpretation can be found. Nonetheless, we know that we can consider the signal as approximately stationary around a given time τ over a timescale τ_s (depending itself on τ): this is the same condition controlling the validity of the functional expansion Eq. (29).

In a given signal, different stationary time scales exist as we discussed already in Sec. III B 2. Figure 10 rep-

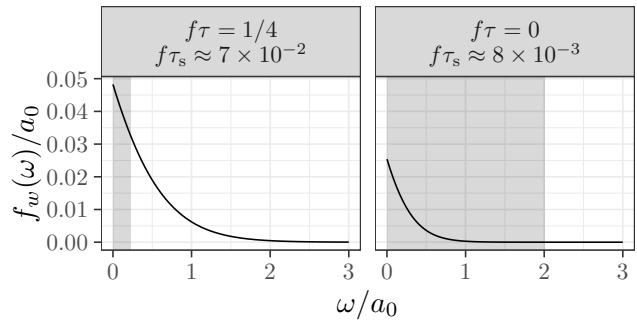


FIG. 10: Gaussian average of the Wigner function over a window given by τ_s such that $|a/\delta a| \leq 1/20$ for the sine case where $a_0 = a_1$, and $2\pi f/a_0 = 1/5$. To have a consistent time-frequency representation, we need to perform another Gaussian average of typical spread given by the shaded area which depends on τ_s . A particle picture is meaningful only above this frequency threshold.

resents the (Gaussian) average of the Wigner function around a time τ with a time window of typical width τ_s : only a section is represented (it is sufficient since we are approximately stationary) and corresponds to the averaged energy distribution $f_w(\omega)$. To be consistent and respect the Heisenberg time-frequency indeterminacy, a (Gaussian) average should be performed in frequency: this frequency window is the orange area in Fig. 10 where two extreme cases are shown :

- At the maximum of acceleration (where the adiabatic regime is valid, $f\tau = 1/4$), the distribution $f_w(\omega)$ is a thermal distribution at a temperature around a_τ . The frequency average is such that the overall time-frequency response of a detector with a response function of width τ_s around $f\tau = 1/4$ will be a stationary thermal distribution. We can then reconstruct in this time-frequency domain a uniformly accelerated particle picture.
- At lower accelerations, the distribution $f_w(\omega)$ looks thermal but has to be averaged over a very large frequency domain compared to its typical width. This is a consequence of the very low stationary timescale there. In this case, the only meaningful particle picture that can be constructed is at very high frequencies and matches one of an inertial response. This follows the intuition that high-frequency modes are equal to inertial modes.

In the end, the main lesson from this discussion is that particles emerge from the signal and applying a time-frequency analysis seems the most appropriate to tackle the issue of particle reconstruction and to link the operational and many-body definitions.

VI. CONCLUSION

In this paper, we introduced a signal processing time-frequency approach to the problem of detectors in motion in relativistic quantum field theory. It offers a natural and synthetic framework to analyze non-stationary trajectories. We provided a detailed analysis of the adiabatic regime, its corrections and its breakdown. We then moved on to study how excitations are probed by a moving detector, focusing for clarity on Gaussian states. The structure of the Wigner function can be completely understood using simple approximation schemes. Beside recovering time-frequency special relativistic behaviors in general frames, we were able to analyze how wavepackets and their coherence properties are transformed by the motion of the detector.

We finally used our analysis of excitation and motion to discuss how time-frequency analysis provides a promising approach to clarify conceptual questions behind the problem of moving detectors, especially concerning the definitions of a notion of particles. Indeed, time-frequency allows to define a notion of relative stationary timescales over the signal, permitting than to locally link the operational and many-body definitions of particles.

Apart from those conceptual questions, this time-frequency signal processing approach opens up many in-

teresting perspectives to sharpen our understanding of relativistic detectors. Indeed, a natural generalization is to analyze higher order correlation functions, which play an important role in quantum optics. This would allow to understand from first principles the interplay between entanglement [38, 39], which is encoded in the second order correlation function, and motion in a completely relativistic setting. Moreover, one of the main challenge is to have an experimental access to the Wigner function. Measuring the Wigner is traditionally done through interferometric setup like the Hong-Ou-Mandel experiment. This then demands to properly analyze those interferometric experiments when probed by a moving detector. Finally, the same approach could be generalized to curved spacetime, allowing again to understand the response of detector in non stationary spacetime situations like the formation of black holes by a collapsing star or the effect of gravitation on the entanglement of quantum systems.

Acknowledgments

We thank P. Degiovanni and G. Fève for useful discussions. We also thank J.-M. Raimond for useful remarks on our manuscript.

-
- [1] S. Hollands and K. Sanders, *Entanglement measures and their properties in quantum field theory*, vol. 34. Springer, 2018.
 - [2] E. Witten, “Notes on Some Entanglement Properties of Quantum Field Theory,” *Rev. Mod. Phys.* **90** (2018), no. 4, 045003, [arXiv:1803.04993](https://arxiv.org/abs/1803.04993).
 - [3] S. W. Hawking, “Particle creation by black holes,” *Communications in mathematical physics* **43** (1975), no. 3, 199–220.
 - [4] W. G. Unruh, “Notes on black-hole evaporation,” *Physical Review D* **14** (1976), no. 4, 870.
 - [5] S. Schlicht, “Considerations on the Unruh effect: Causality and regularization,” *Classical and Quantum Gravity* **21** (2004), no. 19, 4647.
 - [6] P. Grove and A. C. Ottewill, “Notes on particle detectors,” *Journal of Physics A: Mathematical and General* **16** (1983), no. 16, 3905.
 - [7] D. Kothawala and T. Padmanabhan, “Response of Unruh–DeWitt detector with time-dependent acceleration,” *Physics Letters B* **690** (2010), no. 2, 201–206.
 - [8] J. Doukas, S.-Y. Lin, B. Hu, and R. B. Mann, “Unruh effect under non-equilibrium conditions: oscillatory motion of an Unruh–DeWitt detector,” *Journal of High Energy Physics* **2013** (2013), no. 11, 119.
 - [9] A. Satz, “Then again, how often does the Unruh–DeWitt detector click if we switch it carefully?,” *Classical and Quantum Gravity* **24** (2007), no. 7, 1719.
 - [10] C. J. Fewster, B. A. Juárez-Aubry, and J. Louko, “Waiting for Unruh,” *Classical and Quantum Gravity* **33** (2016), no. 16, 165003.
 - [11] R. J. Glauber, “Coherent and incoherent states of the radiation field,” *Physical Review* **131** (1963), no. 6, 2766.
 - [12] R. J. Glauber, “The quantum theory of optical coherence,” *Physical Review* **130** (1963), no. 6, 2529.
 - [13] E. Bocquillon, V. Freulon, F. D. Parmentier, J.-M. Berroir, B. Plaçais, C. Wahl, J. Rech, T. Jonckheere, T. Martin, C. Grenier, *et al.*, “Electron quantum optics in ballistic chiral conductors,” *Annalen der Physik* **526** (2014), no. 1-2, 1–30.
 - [14] D. W. Sciama, P. Candelas, and D. Deutsch, “Quantum field theory, horizons and thermodynamics,” *Advances in Physics* **30** (1981), no. 3, 327–366.
 - [15] S. Takagi, “Vacuum Noise and Stress Induced by Uniform Acceleration/Hawking-Unruh Effect in Rindler Manifold of Arbitrary Dimension,” *Progress of Theoretical Physics Supplement* **88** (1986) 1–142.
 - [16] P. Flandrin, *Time-frequency/time-scale analysis*, vol. 10. Academic press, 1998.
 - [17] E. Wigner, “E. Wigner, *Phys. Rev.* 40, 749 (1932).,” *Phys. Rev.* **40** (1932) 749.
 - [18] S. Haroche and J.-M. Raimond, *Exploring the quantum: atoms, cavities, and photons*. Oxford university press, 2006.
 - [19] D. Ferraro, A. Feller, A. Ghibaudo, E. Thibierge, E. Bocquillon, G. Fève, C. Grenier, and P. Degiovanni, “Wigner function approach to single electron coherence in quantum Hall edge channels,” *Physical Review B* **88** (2013), no. 20, 205303.
 - [20] B. Roussel, C. Cabart, G. Fève, E. Thibierge, and P. Degiovanni, “Electron quantum optics as quantum

- signal processing,” *physica status solidi (b)* **254** (2017), no. 3, 1600621.
- [21] B. F. Svaiter and N. F. Svaiter, “Inertial and noninertial particle detectors and vacuum fluctuations,” *Physical Review D* **46** (1992), no. 12, 5267.
- [22] R. F. Streater and A. S. Wightman, *PCT, spin and statistics, and all that*. Princeton University Press, 2016.
- [23] P. Langlois, “Causal particle detectors and topology,” *Annals of Physics* **321** (2006), no. 9, 2027–2070.
- [24] J. Louko and A. Satz, “How often does the Unruh–DeWitt detector click? Regularization by a spatial profile,” *Classical and Quantum Gravity* **23** (2006), no. 22, 6321.
- [25] N. Obadia and M. Milgrom, “Unruh effect for general trajectories,” *Physical Review D* **75** (2007), no. 6, 065006.
- [26] D. Buchholz and J. Schlemmer, “Local temperature in curved spacetime,” *Classical and Quantum Gravity* **24** (2007), no. 7, F25.
- [27] D. Buchholz and C. Solveen, “Unruh effect and the concept of temperature,” arXiv preprint arXiv:1212.2409 (2012).
- [28] C. Barcelo, S. Liberati, S. Sonego, and M. Visser, “Minimal conditions for the existence of a Hawking-like flux,” *Physical Review D* **83** (2011), no. 4, 041501(R).
- [29] L. C. Barbado and M. Visser, “Unruh-DeWitt detector event rate for trajectories with time-dependent acceleration,” *Physical Review D* **86** (2012), no. 8, 084011.
- [30] A. Higuchi, G. E. A. Matsas, and C. B. Peres, “Uniformly accelerated finite-time detectors,” *Physical Review D* **48** (1993), no. 8, 3731.
- [31] L. Sriramkumar and T. Padmanabhan, “Finite-time response of inertial and uniformly accelerated Unruh-DeWitt detectors,” *Classical and Quantum Gravity* **13** (1996), no. 8, 2061.
- [32] K. Lochan and T. Padmanabhan, “Inertial nonvacuum states viewed from the Rindler frame,” *Physical Review D* **91** (2015), no. 4, 044002.
- [33] T. Padmanabhan, “General covariance, accelerated frames and the particle concept,” *Astrophysics and Space Science* **83** (1982), no. 1-2, 247–268.
- [34] L. Sriramkumar and T. Padmanabhan, “Probes of the vacuum structure of quantum fields in classical backgrounds,” *International Journal of Modern Physics D* **11** (2002), no. 01, 1–34.
- [35] A. Ashtekar and A. Magnon, “Quantum fields in curved space-times,” *Proceedings of the Royal Society of London. A. Mathematical and Physical Sciences* **346** (1975), no. 1646, 375–394.
- [36] R. Haag, *Local Quantum Physics: Fields, Particles, Algebras (Theoretical and Mathematical Physics)*. Springer, 1996.
- [37] P. Borgnat, P. Flandrin, P. Honeine, C. Richard, and J. Xiao, “Testing stationarity with surrogates: A time-frequency approach,” *IEEE Transactions on Signal Processing* **58** (2010), no. 7, 3459–3470.
- [38] I. Fuentes-Schuller and R. B. Mann, “Alice falls into a black hole: entanglement in noninertial frames,” *Physical review letters* **95** (2005), no. 12, 120404.
- [39] D. Su and T. C. Ralph, “Decoherence of the radiation from an accelerated quantum source,” *Physical Review X* **9** (2019), no. 1, 011007.

Appendix A: Wigner function of a discontinuous acceleration

We will consider the case where an observer is going from an inertial phase to a uniformly accelerated phase at acceleration a . Its trajectory in its proper time can be written as

$$x(\tau) = \begin{cases} (\tau, 0) & \text{if } \tau \leq 0, \\ (a^{-1} \sinh a\tau, a^{-1}(\cosh a\tau - 1)) & \text{if } \tau \geq 0. \end{cases} \quad (\text{A1})$$

We see that this expression has a discontinuity in the second derivative of $x(\tau)$. We expect the expression of $G(\tau + v/2, \tau - v/2)$ to have discontinuities in second- or higher-order derivatives. Since algebraic high-frequency behaviors of the Fourier transform are determined by those discontinuities, we will take some care to analyze them. For this we will rewrite

$$G(\tau + v/2, \tau - v/2) = f_\tau(v) + g_\tau(v), \quad (\text{A2})$$

where f contains the lower-order discontinuities of G , and g may contain higher-order discontinuities. While the function f is arbitrary, its high-frequency behavior only depends on the discontinuities, and not on the precise details of f .

In this case, G has discontinuities at $v = \pm 2\tau$. Since $G(\tau + v/2, \tau - v/2)$ is even in v , we will consider only the case $v \geq 0$. We will choose for f an even truncated polynomial, to take into account this symmetry

$$f_\tau(v) = \frac{\alpha}{n!} (v - 2\tau)^n (v + 2\tau)^n \Pi_{[-2\tau, 2\tau]}(v), \quad (\text{A3})$$

where n is the order of the discontinuity, Π is the gate function and α is such that f captures the discontinuities of G ,

$$\partial_v^n G|_{v=2|\tau|^+} - \partial_v^n G|_{v=2|\tau|^-} = \partial_v^n f_\tau|_{v=2|\tau|^+} - \partial_v^n f_\tau|_{v=2|\tau|^-}. \quad (\text{A4})$$

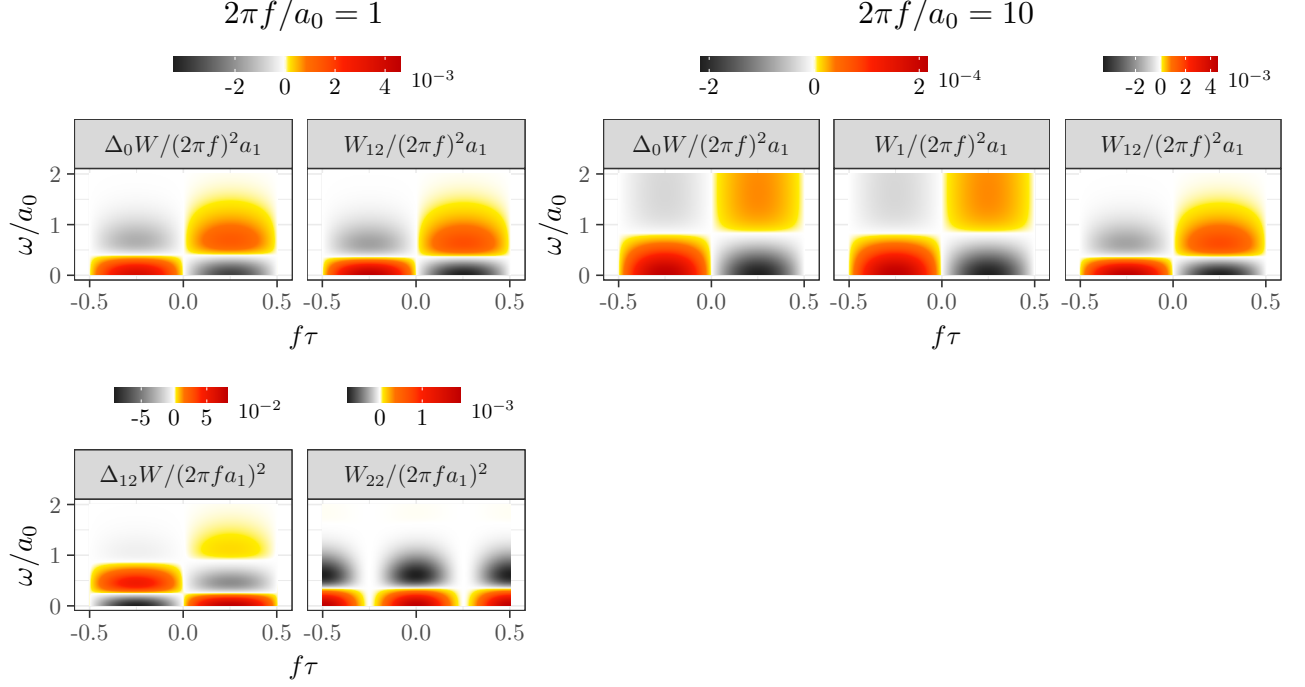


FIG. 11: Different breakdowns of adiabatic expansions when the first derivative \dot{a} is small for a sinusoidal acceleration. In these plots we keep $2\pi f a_1/a_0 = 10^{-2}$. On the left, the frequency being of the order of a_0 , the adiabatic development breaks down after the correction in \ddot{a} . On the right, the frequency is much higher than a_0 . While the perturbative expansion works perfectly well, the adiabatic development breaks down, even at first order. We see also that corrections are important outside of the thermal bandwidth in this case.

For $\tau \geq 0$, the discontinuity happens in the second derivative of G . After performing the Fourier transform of the corresponding $f\tau$, we find that the high-frequency behavior is expressed as

$$\Delta W(\tau, \omega) \simeq -\frac{1}{4\pi^2} \frac{a^4}{8 \sinh^2 a\tau} \frac{\sin 2\omega\tau}{\omega^3}. \quad (\text{A5})$$

For $\tau \leq 0$, G has a discontinuity in its third derivative. The same technique gives the result

$$\Delta W(\tau, \omega) \simeq -\frac{1}{4\pi^2} \frac{a^2}{16\tau^3} \frac{\cos 2\omega\tau}{\omega^4}. \quad (\text{A6})$$

Appendix B: Adiabatic regime

In this appendix, we will give some further details about the adiabatic development. We will start by the functional development, up to first order in Appendix B1. We will then focus on the derivative development in Appendix B2. The validity of the different developments can be seen on Fig. 11.

1. Functional development

In order to perform the derivative development, we will write the acceleration as

$$a(\tau + v) \simeq a(\tau) + \delta_\tau a(v). \quad (\text{B1})$$

We will see that, provided that $\delta_\tau a(v) \ll a(\tau)$ for $|v| < \tau_s$ and $a\tau_s \gg 1$, this development is valid. We can rewrite the first order term as

$$W_1(\tau, \omega) = \frac{1}{4\pi^2} \int \frac{a(\tau)^3}{4 \sinh^3(a(\tau)v/2)} \int_{-v/2}^{v/2} \sinh(a(\tau)v') \delta_\tau A(v') dv' e^{i\omega v} dv, \quad (\text{B2})$$

with $\delta_\tau A(v) = \int_0^v \delta_\tau a(v') dv'$.

From this development, we can see that the first-order term only depends on the odd part of $\delta_\tau A$, and thus the even part of $\delta_\tau a$. Furthermore, if $\delta_\tau A$ has a polynomial behavior, the integrand has an exponential cut-off in $|v|$. Provided that $\delta_\tau a$ is small enough compared to $a(\tau)$ over a scale $\tau_s \gg a(\tau)^{-1}$, this first-order correction will be small compared to the thermal behavior.

Since this term is a linear functional in $\delta_\tau a$, we can treat it through Fourier analysis. Since we are only sensitive to the even part of $\delta_\tau a$, we can set

$$\delta_\tau a(v) = a_1(\tau)(\cos(2\pi f v) - 1). \quad (\text{B3})$$

In this case, we find that

$$W_1 = \frac{a_1}{4\pi^2} \left[\frac{1}{1 + (2\pi f/a_\tau)^2} \frac{g_+ + g_-}{2} - \frac{\omega/2\pi f}{1 + (2\pi f/a_\tau)^2} (g_+ - g_-) + \frac{2\pi}{a_\tau} \omega g_0 - g_0 \right]. \quad (\text{B4})$$

If $2\pi f \ll a_\tau$, we can use a perturbative development

$$W_1(\tau, \omega) = \frac{a_1}{4\pi^2} \left(\frac{2\pi f}{a(\tau)} \right)^2 \left[-1 + \frac{2\pi}{a(\tau)} \omega \partial_x + \frac{1}{2} (\pi \partial_x)^2 - \frac{1}{3} \frac{\omega}{a(\tau)} (\pi \partial_x)^3 \right] g \left(\frac{2\pi}{a(\tau)} \omega \right), \quad (\text{B5})$$

with $g(x) = x/(\exp(x) - 1)$.

This correction is vanishing quadratically as frequency is lowered. Furthermore, all the corrective terms act in the thermal bandwidth. The first two terms can be seen as a correction to the thermal state by a difference of temperature $-a_0(2\pi f/a(\tau))^2$. This correction can be interpreted as a averaging effect due to the even part of the acceleration.

On the contrary, when $2\pi f \gg a(\tau)$, we can approximate the corrective term with

$$W_1(\tau, \omega) = \frac{a_1}{4\pi^2} \left[-g_0 + \frac{2\pi}{a_1} \omega g'_0 \right] + \frac{a_1}{4\pi^2} \frac{g_-}{1 + (2\pi f/a(\tau))^2} \left(\frac{1}{2} + \frac{\omega}{2\pi f} \right). \quad (\text{B6})$$

The first term corresponds to a shift of the temperature to the average value of $\delta_\tau a$. At high frequencies, the temperature is thus blurred by the average behavior. The second term is exponentially small for frequencies higher than πf . Below πf , it behaves like the quadratic form:

$$\frac{a_0}{4\pi^2} \frac{a(\tau)}{4f} \left(1 - \left(\frac{\omega}{\pi f} \right)^2 \right). \quad (\text{B7})$$

Thus, this correction to the average thermal behavior has a bandwidth much larger than the one of thermal fluctuations.

2. Derivative development

We saw in the previous development that the linear term in $\delta_\tau a$ only depends on the even part of $\delta_\tau a$. Since in the adiabatic regime the frequencies contained in $a(\tau)$ around a window of size τ_s are expected to be sufficiently low compared to the $a(\tau)$, we should have the splitting of order $\dot{a}(\tau) \gg \ddot{a}(\tau)$, and higher order derivative should be negligible in front of those terms. As such, we will develop to the terms $\ddot{a}(\tau)/a(\tau)^3$ and $\dot{a}(\tau)^2/a(\tau)^4$.

The term in $\ddot{a}(\tau)/a(\tau)^3$ reads

$$W_{12}(\tau, \omega) = -\frac{1}{4\pi^2} \frac{\ddot{a}(\tau)}{a(\tau)^2} \left[-1 + \frac{2\pi}{a(\tau)} \omega \partial_x + \frac{1}{2} (\pi \partial_x)^2 - \frac{1}{3} \frac{\omega}{a(\tau)} (\pi \partial_x)^3 \right] g \left(\frac{2\pi}{a(\tau)} \omega \right). \quad (\text{B8})$$

We recover here the approximation of the linear term in case of small frequencies.

The terms in $\dot{a}(\tau)^2/a(\tau)^4$ reads

$$W_{22}(\tau, \omega) = \frac{2}{3\pi^2} \frac{\dot{a}(\tau)^2}{a(\tau)^3} \left[-1 + \frac{2\pi}{a(\tau)} \omega \partial_x + \left(\left(\frac{\omega}{2a(\tau)} \right)^2 + \frac{5}{8} \right) (\pi \partial_x)^2 \right] g \left(\frac{2\pi}{a(\tau)} \omega \right). \quad (\text{B9})$$

In this case, the first two terms can also be seen as a small thermal shift by $8\dot{a}^2/3a^3$.

Appendix C: Fock and mono-chromatic coherent state

In this appendix, we present the computation of the Wigner function of a mono-chromatic coherent state and Fock state. First let's suppose we have a single mode coherent state $|\alpha_{\mathbf{p}}\rangle$. Given the commutation relation that we have, the overlap between two coherent states is given by

$$\langle \alpha_{\mathbf{p}} | \alpha_{\mathbf{p}'} \rangle = 2\omega_{\mathbf{p}} (2\pi)^3 \delta(\mathbf{p} - \mathbf{p}'). \quad (\text{C1})$$

Then the first order coherent function can be computed directly has

$$\langle \alpha_{\mathbf{p}} | \phi(\tau) \phi(\tau') | \alpha_{\mathbf{p}} \rangle = \langle 0 | \phi(\tau) \phi(\tau') | 0 \rangle + \alpha_{\mathbf{p}}^2 e^{-i[\omega_{\mathbf{p}}(t+t') - \mathbf{p} \cdot (\mathbf{x} + \mathbf{x}')] } + \alpha_{\mathbf{p}} \bar{\alpha}_{\mathbf{p}} e^{i[\omega_{\mathbf{p}}(t-t') - \mathbf{p} \cdot (\mathbf{x} - \mathbf{x}')] } + \text{h.c.} \quad (\text{C2})$$

where (t, \mathbf{x}) are functions of the proper time τ .

Let's check quickly what we obtain for inertial trajectories. For one with zero velocity $(\tau, 0)$, we have

$$W_{|\alpha_{\mathbf{p}}\rangle}(\tau, \omega) = W_{|0\rangle}(\tau, \omega) + |\alpha_{\mathbf{p}}|^2 (\delta(\omega + \omega_{\mathbf{p}}) + \delta(\omega - \omega_{\mathbf{p}})) + 2\Re(\alpha_{\mathbf{p}}^2 e^{-2i\omega_{\mathbf{p}}\tau}) \delta(\omega). \quad (\text{C3})$$

For an inertial observer with velocity \mathbf{v} which then has the trajectory $(\gamma\tau, \gamma v\tau)$, the Wigner function remains the same except that the frequency of the coherent state is Doppler shifted to $\omega_{\mathbf{p}}^{\mathbf{y}} = \gamma[\omega_{\mathbf{p}} - \mathbf{v} \cdot \mathbf{p}]$.

Now consider the uniformly accelerated trajectory $(a^{-1} \sinh a\tau, a^{-1}(\cosh a\tau - 1))$. From (C2) we have to compute two different integrals:

$$W_{|\alpha_{\mathbf{p}}\rangle}^a(\tau, \omega) = W_{|0\rangle}^a(\tau, \omega) + \alpha_{\mathbf{p}}^2 I_1^+(\tau, \omega) + \alpha_{\mathbf{p}} \bar{\alpha}_{\mathbf{p}} (I_2^+(\tau, \omega) + I_2^-(\tau, \omega)) + \bar{\alpha}_{\mathbf{p}}^2 I_1^-(\tau, \omega) \quad (\text{C4})$$

with

$$I_1^+(\tau, \omega) = e^{-2ip} \int_{\mathbb{R}} e^{-2i[\omega_p a^{-1} \sinh a\tau - p_x a^{-1} \cosh a\tau] \cosh av/2} e^{i\omega v} dv \quad (\text{C5a})$$

$$I_2^+(\tau, \omega) = \int_{\mathbb{R}} e^{2i[\omega_p a^{-1} \cosh a\tau - p_x a^{-1} \sinh a\tau] \sinh av/2} e^{i\omega v} dv. \quad (\text{C5b})$$

Since $\omega_p = p$, we can say that the function $f(\tau) = 2[\omega_p a^{-1} \cosh a\tau \mp p a^{-1} \sinh a\tau]$ is always positive and independent of v . Here we choose the coherent state momentum to be in the same direction as the accelerated observer, $p_x > 0$. The case with opposite momentum is treated in the same way. Furthermore, the phase in front of the integral of I^+ can be absorbed by a change of phase of the coherent state and will then be omitted in the following. Thus we have to compute

$$I_1^{\pm}(\tau, \omega) = \int_{\mathbb{R}} e^{\pm if(\tau) \cosh av/2} e^{i\omega v} dv \quad (\text{C6a})$$

$$I_2^{\pm}(\tau, \omega) = \int_{\mathbb{R}} e^{\pm if(\tau) \sinh av/2} e^{i\omega v} dv. \quad (\text{C6b})$$

The first integrals corresponds exactly to an integral representation of the Hankel functions defined as

$$H_{\nu}^{(1)}(x) = \frac{e^{-\frac{\nu\pi i}{2}}}{i\pi} \int_{\mathbb{R}} e^{ix \cosh t - \nu t} dt \text{ for } x > 0, |\Re(\nu)| < 1 \quad (\text{C7a})$$

$$H_{\nu}^{(2)}(x) = -\frac{e^{\frac{\nu\pi i}{2}}}{i\pi} \int_{\mathbb{R}} e^{-ix \cosh t - \nu t} dt \text{ for } x > 0, |\Re(\nu)| < 1. \quad (\text{C7b})$$

So we directly have

$$I_1^+(\tau, \omega) = \frac{2i\pi}{a} e^{\frac{\omega\pi}{a}} H_{-2i\omega/a}^{(1)}(f(\tau)) = \frac{4}{a} K_{-2i\omega/a}(-if(\tau)) \quad (\text{C8a})$$

$$I_1^-(\tau, \omega) = -\frac{2i\pi}{a} e^{-\frac{\omega\pi}{a}} H_{-2i\omega/a}^{(2)}(f(\tau)) = \frac{4}{a} K_{2i\omega/a}(if(\tau)) \quad (\text{C8b})$$

where the special functions K_{ν} are modified Bessel functions of the second kind. In short

$$I_1^{\pm}(\tau, \omega) = \frac{4}{a} K_{\mp 2i\omega/a}(\mp if(\tau)). \quad (\text{C9})$$

The second integral is also related to Hankel functions or Bessel functions. By deforming the contour of integration by a translation of $\pm i\pi/2$, we have

$$\int_{\mathbb{R}} e^{ix \sinh t + i\omega t} dt = \int_{\mathbb{R}} e^{ix \sinh(t+i\pi/2) + i\omega(t+i\pi/2)} dt = e^{-\frac{\omega\pi}{2}} \int_{\mathbb{R}} e^{-x \cosh t + i\omega t} dt = 2e^{-\frac{\omega\pi}{2}} K_{i\omega}(x) \quad (\text{C10})$$

so that

$$I_2^\pm(\tau, \omega) = \frac{4}{a} e^{\mp \frac{\omega\pi}{a}} K_{2i\omega/a}(f(\tau)). \quad (\text{C11})$$

The case of Fock states are treated in the same way. In fact, all computations have already been done in the case of coherent states, see (C11). For a single mode Fock state

$$\langle n_{\mathbf{p}} | \phi(\tau) \phi(\tau') | n_{\mathbf{p}} \rangle = \langle 0 | \phi(\tau) \phi(\tau') | 0 \rangle + n_{\mathbf{p}} \left(e^{i[\omega_{\mathbf{p}}(t-t') - \mathbf{p} \cdot (\mathbf{x} - \mathbf{x}')] } + e^{-i[\omega_{\mathbf{p}}(t-t') - \mathbf{p} \cdot (\mathbf{x} - \mathbf{x}')] } \right). \quad (\text{C12})$$

We can check directly that

$$W_{|n_{\mathbf{p}}\rangle}(\tau, \omega) = W_{|0\rangle}(\tau, \omega) + n_{\mathbf{p}} (\delta(\omega + \omega_{\mathbf{p}}) + \delta(\omega - \omega_{\mathbf{p}})) \quad (\text{C13a})$$

$$W_{|n_{\mathbf{p}}^{\mathbf{v}}\rangle}(\tau, \omega) = W_{|0\rangle}(\tau, \omega) + n_{\mathbf{p}} (\delta(\omega + \omega_{\mathbf{p}}^{\mathbf{v}}) + \delta(\omega - \omega_{\mathbf{p}}^{\mathbf{v}})) \quad (\text{C13b})$$

$$W_{|n_{\mathbf{p}}^a\rangle}(\tau, \omega) = W_{|0\rangle}^a(\tau, \omega) + n_{\mathbf{p}} (I_2^+(t, \omega) + I_2^-(t, \omega)). \quad (\text{C13c})$$

Appendix D: Gaussian and stationary phase approximations

In this appendix, we give a more detailed analysis of the two approximation schemes used in Sec. IV to understand the qualitative form of the Wigner function of Gaussian wavepackets.

1. Gaussian approximation

For a general trajectory, computing analytically the Wigner function is not possible. Nonetheless, meaningful information can be already uncovered by resorting to a Gaussian approximation. One has to approximate the wavefunction $\Phi_\alpha(\tau)$ has a Gaussian in time around its maximum value. From

$$\Phi_\alpha(\tau) = \sqrt{\frac{p_0}{(2\pi\sigma_x^2)^{1/2}}} e^{-[f_-(\tau) + x_0]^2 / 4\sigma_x^2} e^{-ip_0[f_-(\tau) + x_0]}, \quad (\text{D1})$$

let's do an expansion around the maximum reached at time τ_r : $\int_0^{\tau_r} \exp(-A(u)) du = x_0$. We now expand around this maximum. Thus,

$$f_-(\tau_r + v) = x_0 + D_r v - \frac{1}{2} a_r D_r v^2 \quad (\text{D2a})$$

$$f_-(\tau_r + v)^2 = x_0^2 + 2x_0 D_r v + D_r (D_r - x_0 a_r) v^2 \quad (\text{D2b})$$

with $D_r = e^{-A(\tau_r)}$ is the gravitational redshift shift, as we will see. We can start by approximating the wavefunction as a Gaussian. We have

$$\Phi(\tau_r + v) = \sqrt{\frac{p_0}{(2\pi\sigma_x^2)^{1/2}}} \exp\left(-\frac{D_r^2}{4\sigma_x^2} v^2 + \frac{i}{2} p_0 a_r D_r v^2 - ip_0 D_r v\right). \quad (\text{D3})$$

We recognize here a Gaussian linear chirp, centered around frequency $\omega_r = D_r p_0$, time t_r and with a chirp rate $-\omega_r a_r$. To this order, we find that the Wigner function associated with the $\Phi^* \Phi$ and the $\Phi \Phi + \Phi^* \Phi^*$ terms are respectively given by

$$W_{\Phi_\alpha \Phi_\alpha^*}(\tau, \omega) = \frac{2p_0}{D_r} \exp\left(-\frac{D_r^2}{2\sigma_x^2} (\tau - \tau_r)^2\right) \exp\left(-\frac{1}{2} \frac{4\sigma_x^2}{D_r^2} (\omega - \omega_r (1 - a_r (\tau - \tau_r)))^2\right) \quad (\text{D4a})$$

$$W_{\Phi_\alpha \Phi_\alpha}(\tau, \omega) = \Re \frac{2}{\sqrt{D_r^2 - 2ia_r \omega_r \sigma_x^2}} \exp\left(-\frac{D_r^2}{2\sigma_x^2} (\tau - \tau_r)^2 - \frac{1}{2} \frac{4\sigma_x^2}{D_r^2 + 4a_r^2 \omega_r^2} \omega^2\right) \exp\left(i\omega_r a_r \left((\tau - \tau_r)^2 + \frac{\omega^2}{D_r^4 / 4\sigma_x^4 + a_r^2 \omega_r^2}\right)\right) \exp(2i\omega_r (\tau - \tau_r)). \quad (\text{D4b})$$

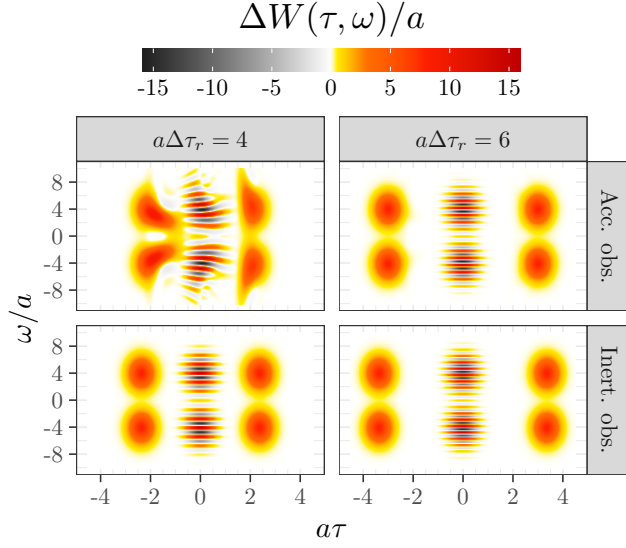


FIG. 12: Comparison of the signal received from a superposition of coherent states for a uniformly accelerated (top row) and inertial detector (bottom row). $\Delta\tau_r$ is the time difference between the two members of the superposition in the accelerated frame. The time dilation for this twin paradox configuration is clear. (Parameters : Total time $a\tau_{\text{acc}} = 4$, transitions at $\tau = -2, -1, 1, 2$ (proper time), $p_0/a = 4$, $a\sigma_x = 1/3$.)

2. Stationary phase approximation

The stationary phase approximation allows to write the approximate form:

$$W(\tau, \omega) = \sum_s \frac{(8\pi)^{1/2}}{|\partial_v^2 \Phi(\tau_s; \tau, \omega)|^{1/2}} A(\tau_s; \tau) \cos \left(\Phi(\tau_s; \tau, \omega) + \frac{\pi}{4} \text{sgn} \partial_v^2 \Phi(\tau_s; \tau, \omega) \right) \quad (\text{D5})$$

On the points where the stationary phase is valid, the Wigner function (the term $\Phi_\alpha(t, \mathbf{x})\Phi_\alpha^*(t', \mathbf{x}') + \text{h.c.}$) of a Gaussian coherent state probed by a uniformly accelerated observer is:

$$W_{\Phi_\alpha \Phi_\alpha^*}(\tau, \omega) = \frac{2p_0}{\sigma_x} \sqrt{\frac{2}{a\sqrt{\omega^2 - \omega^2(\tau)}}} \exp \left(-\frac{1}{2(ap_0\sigma_x)^2} [(\omega - \omega_r)^2 + (\omega - \omega(\tau))(\omega + \omega(\tau))] \right) \cos \left(2a^{-1}\sqrt{\omega^2 - \omega^2(\tau)} - 2a^{-1}\omega \text{argcosh} \left(\frac{\omega}{\omega(\tau)} \right) + \frac{\pi}{4} \right) \quad (\text{D6})$$

Since far away from the instantaneous frequency curve the Wigner function is decreasing in a Gaussian way, it is meaningful to expand the argument of the cosine function in $\omega/\omega(\tau)$. Then we have the approximate form

$$W_{\Phi_\alpha \Phi_\alpha^*}(\tau, \omega) = \frac{2p_0}{\sigma_x} \sqrt{\frac{2}{a\sqrt{\omega^2 - \omega^2(\tau)}}} \exp \left(-\frac{(\omega - \omega_r)^2 + [\omega - \omega(\tau)][\omega + \omega(\tau)]}{2(ap_0\sigma_x)^2} \right) \cos \left(\frac{2\omega}{a} [1 - \ln 2\omega/\omega(\tau)] + \frac{\pi}{4} \right). \quad (\text{D7})$$

The logarithmic correction $\omega \ln \omega/p_0$ can also be neglected at first order. This gives the final approximate form

$$W_{\Phi_\alpha \Phi_\alpha^*}(\tau, \omega) = \frac{2p_0}{\sigma_x} \sqrt{\frac{2}{a\sqrt{\omega^2 - \omega^2(\tau)}}} \exp \left(-\frac{(\omega - \omega_r)^2 + [\omega - \omega(\tau)][\omega + \omega(\tau)]}{2(ap_0\sigma_x)^2} \right) \cos \left(2[1 - \ln 2] \frac{\omega}{a} - 2\omega\tau + \frac{\pi}{4} \right). \quad (\text{D8})$$